DESIGN AND TESTING OF A TRACTION/DISTRACTION KNEE BRACE

A Thesis Submitted to the College of

Graduate and Postdoctoral Studies

In Partial Fulfillment of the Requirements

For the Degree of Master of Science

In the Department of Mechanical Engineering

University of Saskatchewan

Saskatoon

By

TIMOTHY JAMES GADZELLA

Permission to Use

In presenting this thesis/dissertation in partial fulfillment of the requirements for a Postgraduate degree from the University of Saskatchewan, I agree that the Libraries of this University may make it freely available for inspection. I further agree that permission for copying of this thesis/dissertation in any manner, in whole or in part, for scholarly purposes may be granted by the professor or professors who supervised my thesis/dissertation work or, in their absence, by the Head of the Department or the Dean of the College in which my thesis work was done. It is understood that any copying or publication or use of this thesis/dissertation or parts thereof for financial gain shall not be allowed without my written permission. It is also understood that due recognition shall be given to me and to the University of Saskatchewan in any scholarly use which may be made of any material in my thesis/dissertation.

DISCLAIMER

Reference in this thesis/dissertation to any specific commercial products, process, or service by trade name, trademark, manufacturer, or otherwise, does not constitute or imply its endorsement, recommendation, or favoring by the University of Saskatchewan. The views and opinions of the author expressed herein do not state or reflect those of the University of Saskatchewan, and shall not be used for advertising or product endorsement purposes.

Requests for permission to copy or to make other uses of materials in this thesis/dissertation in whole or part should be addressed to:

Head of the Department of Mechanical Engineering
57 Campus Drive
University of Saskatchewan
Saskatoon, Saskatchewan S7N 5A9
Canada

OR

Dean
College of Graduate and Postdoctoral Studies
University of Saskatchewan
116 Thorvaldson Building, 110 Science Place
Saskatoon, Saskatchewan S7N 5C9
Canada

Abstract

A new knee brace design is required to provide non-surgical distraction of the knee joint for extended periods of time. This knee brace needs to apply traction force to the joint directly, rather than indirectly unloading one compartment. In providing such a design, this research had two objectives: 1) to design a lower-leg knee brace that can apply traction load to the knee; and 2) to test prototypes of these lower-leg knee brace components and relate the traction load to wearer discomfort and interface force.

The first objective was met through prospective analysis and iterative design. A planar finite element (FE) model of the lower leg was used to analyse the effect of knee brace coverage. It was observed that increasing the coverage of the knee brace may reduce interface pressures and concentrations of force. A lower-leg knee brace was designed responding to this model, using fibreglass casts with embedded fasteners to transfer load. Braces were manufactured in three lengths for testing: 3”, 7”, and a combined (“mixed”) design with components from each.

Nine participants were recruited for pilot testing of the lower leg knee brace. A mechanical test frame was built to apply traction load to the participants’ legs through each of the prototype knee braces. The load in the test frame was increased in $3kg_f$ increments as interface force measurements were taken. Participants self-reported their discomfort on an 11-point Likert scale or Numerical Rating Scale (NRS).

Results of the pilot study showed significant differences among the brace designs. The 3” design showed higher NRS scores than the 7” and mixed designs by a full NRS step. Graphical profiles of the interface force suggested that this difference may be the result of higher interface forces distributed across the smaller area of the 3” brace. However, no significant correlation between maximum interface force and self-reported pain was found. Parameters characterizing the shape of the participant’s lower legs indicated that leg shape may influence brace effectiveness.

This study concluded that a rigid knee brace is indeed a valid design, but a longer knee brace interface is required for the anterior surface of the leg to improve comfort. This length may not be required for the posterior surface. Further, this study demonstrated simple relationships among applied load, interface force, and wearer discomfort. Future work will adapt this design to the upper leg and optimize the design to minimize force concentrations at the joints.

Acknowledgments

I would like first and foremost to acknowledge the support of my supervisors, Professors JD Johnston and Allan Dolovich. This thesis is the result of many hours spent in their offices tossing around ideas and drawing inspiration from comic books and movies. Their mentorship, guidance, and willingness to let me explore the fantastic were instrumental to this work. I cannot possibly thank them enough.

I would also like to thank my committee members, Professors Emily McWalter and Joel Lanovaz, for their guidance in this research. I would also like to thank Professor Saija Kontulainen for her guidance in the analysis of our data.

I would like to acknowledge the support of the staff of the Department of Mechanical Engineering, specifically Rob Peace and Mike Miller. I would also like to acknowledge the support of our lab group: Amy, Brennan, Kadin, IBK, Nema, Mahdi, Mehrdad, Lumeng, and Dena.

I am fortunate to have what I can only describe as an army of friends and family who supported my research throughout the past two years. This legion of positivity marches under many banners: they are my parents, my sisters Ehren and KP, the boys of Atlas Company, the cheerful Viking folk of Myrgan Wood, the plucky crew of the Dissonant Heart, and the hit-point sinks of the Harambe's Heroes Guild. They have been marshalled with seemingly unending patience by my fiancée Katie, whose care and attention gave untellable amounts to this thesis. Thank you all for your interest in my work and for giving me the occasional escape by indulging my love of fantasy. You help keep the magic alive.

For Mum and Dad:

something need-to-have.

Table of Contents

List of Figures

List of Tables

List of Abbreviations

ADM – Analog Discovery Module

EKAM – External Knee Adduction Moment

FBPSS – Function-Behaviour-Principle-System-State [design model]

JSW – Joint Space Width

KJD – Knee Joint Distraction

NRS – Numerical Rating Scale

OA - Osteoarthritis

OARSI – Osteoarthritis Research Society International

PPT – Pressure Pain Threshold

RMSE – Root Mean Square Error

WOMAC – Western Ontario and McMaster Universities Osteoarthritis [index]

1 Introduction

Osteoarthritis (OA) is a leading cause of disability, causing growing concern for many Canadians who wish to be active and healthy. According to the Canadian Chronic Disease Surveillance System, 13% of Canadians over the age of 20 years are affected by OA[1]. When the knee joint is affected by OA it may lead to disability and inferior quality of life. Total knee replacements are an option to restore function to those suffering most severely from OA but are only available at the advancing stages of the disease. There are non-surgical treatment methods for knee OA, summarized by the Osteoarthritis Research Society International (OARSI) in their published guidelines[2]. OARSI's panel of experts and patients recommend weight management, strength training, and biomechanical interventions (e.g. knee bracing) as appropriate elements to a complete treatment regime.

The subject of this thesis is the design of knee braces, an example of biomechanical interventions for OA management described in the OARSI guidelines. Evidence is surfacing that indicates that changes to the loads in the knee resulting from joint distraction may be key to delaying the degenerative effects of OA[3-5]. The main goal of this research is to adapt knee brace interface design to address current challenges in surgical methods of providing joint distraction.

Current OA knee braces are "unloaders", creating moments about the knee to limit joint torques that cause joint pain during gait. These braces provide a simple solution to a complicated biomechanical problem but see low long-term compliance due to poor fit and discomfort of the wearer[6]. Instead, knee braces should adapt to directly oppose the forces acting through the knee rather than redistribute them, while simultaneously addressing issues of comfort and compliance. Further, it is desirable to obtain quantitative data relating these parameters for use in engineering models. This research attempts to address each of these problems through the redesign of a lower-leg component to a new knee brace. This knee brace component is assessed by its capability to deliver traction load to a human leg, the behaviour of the mechanical interface between brace and leg, and the resulting comfort of the wearer.

2 Literature Review

2.1 Functional Anatomy of the Knee Joint

The tibiofemoral joint of the human knee is the joint between the three long bones of the lower leg – the tibia, fibula, and femur. These bones meet in the arrangement shown in Figure 2.1, with the tibia and fibula extending distally to meet the tarsal bones of the foot. The femur extends proximally to the hip.

Figure 2.1: Anatomy of the knee joint (excluding patella)[7]

The tibiofemoral joint is contained in a synovial capsule consisting of connective tissue, ligaments, and the femoral-patellar joint (not pictured in the image above). Inside this capsule is fluid that provides lubrication and nutrition to the tissues inside. The capsule includes the collateral ligaments (medial and lateral) and the cruciate ligaments (posterior and anterior). These ligaments hold the bones together and constrain movement as the joint articulates.

The surfaces of the tibia and femur that act as bearing surfaces of the joint are covered by articular cartilage. This soft tissue provides a smooth surface for the bones to pass over with respect to each other. Between the articulating surfaces are the meniscii, small semi-disks of cartilage-like tissue that provide further shock absorption and alignment. Each of these tissues

help provide shock absorption and alignment for the knee joint as it articulates. The health of these tissues directly influences the knee joint's ability to function.

2.2 Osteoarthritis and Knee Joint Distraction

OA is a debilitating disease that affects articulating joints, causing pain and decreasing functionality. The disease is characterized by physiological changes in the muscoloskeletal tissues of the affected joint such as the formation of cysts and bony protrusions (osteophytes), inflammation, degradation of articulating tissues and the closure of the joint space as well as pain[8]. The features of OA are numerous, but all influence the health of the tissues in the affected joint. The prevailing hypothesis is that OA progresses due to an imbalance of damaging and synthetic processes, resulting in tissues that cannot perform[8].

There are a number of metrics for measuring the severity of OA. The Kellgren-Lawrence scale employs radiographic measures to assess the severity of OA based upon features such as narrowing of the joint space width (JSW) and osteophyte formation[9]. Other changes in such as altered bone density and the formation of cysts have also been linked with OA progression[8].

Little is known about the degradation/synthesis mechanism of OA, so most treatments of OA focus on treating the primary symptom (pain) rather than combatting the cause of the disease. One such treatment is joint distraction, in which mechanical force is applied to the joint to separate the articulating surfaces of the bone for brief periods of time. Joint distraction can be applied by hand[10] but is also applied using constant-traction force generating devices[11,12]. In patients with knee OA, knee joint distraction (KJD) has been shown to lessen pain and improve function when coupled with regular physiotherapy[12].

There is reason to believe that joint distraction may have greater effects than reducing pain. Surgical methods of joint distraction in the human ankle[13] and canine models of knee OA[14] have been somewhat successful at restoring function and health to tissues. These studies led to pilot work in using KJD to combat OA in humans.

The first trials in long-term surgical KJD were performed using monotube fixators (typically used for fixing bones in the wrist after fracture). In the pilot study by Intema et al[3], participants with radiologically-confirmed knee OA had two fixators surgically inserted through the soft tissue of the leg into the tibia and femur. These fixators were adjusted to set the endpoints of the

tibia and femur with a JSW of 5mm as confirmed by radiographs. Because these fixators are spring-loaded, participants were able to walk with their full weight on their fixated knee with some degree of compliance (despite the angular position of the knee being fixed). Participants' knees were fixated for approximately two months with intermittent appointments to remove the fixators and flex the knee.

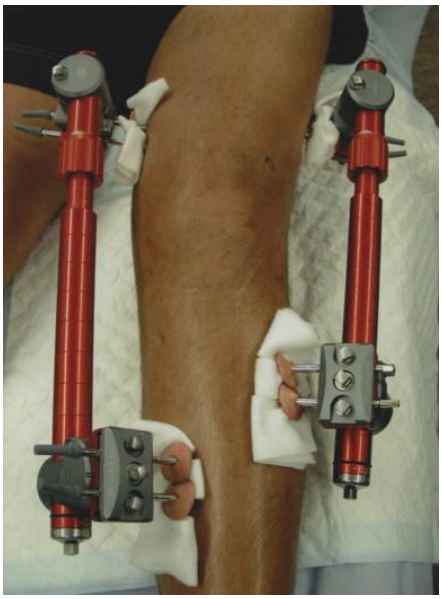

Figure 2.2: Surgically distracted knee with two monotube fixators (medial and lateral), reproduced with permission4

The initial results from this pilot study were extremely promising. Like short-term, non-surgical KJD, pain scores and functionality in the treated joints were improved. Unlike other methods for KJD, physiological changes were observed. Immediately after the distraction protocol, the JSW in the knee compartment most affected by OA was much greater than at baseline. Similarly, the overall JSW in the knee was improved[3]. Other earmarks of OA such as subchondral bone density and the thickness and area coverage of the articular cartilage were also significantly improved by surgical KJD. By changing the method of distraction to allow for long-term manipulation of the joint (as opposed to short bursts in a medical appointment), KJD was able to relieve the symptoms of OA and combat some of the physiological damage from the disease.

Even more impressive are the results of two- and five-year follow-ups to the pilot study. At two-year follow up, WOMAC pain and function scores were still significantly better than baseline (although lower than at 1 year)[4]. Physiological markers such JSW and cartilage coverage and

thickness were also still improved over baseline but lower than at 1-year follow up. Examples of these trends for the most affected compartment (MAC) are demonstrated for thickness of cartilage over bone area, percent of denuded bone, and cartilage thickness over cartilage-covered area in Figure 2.3.

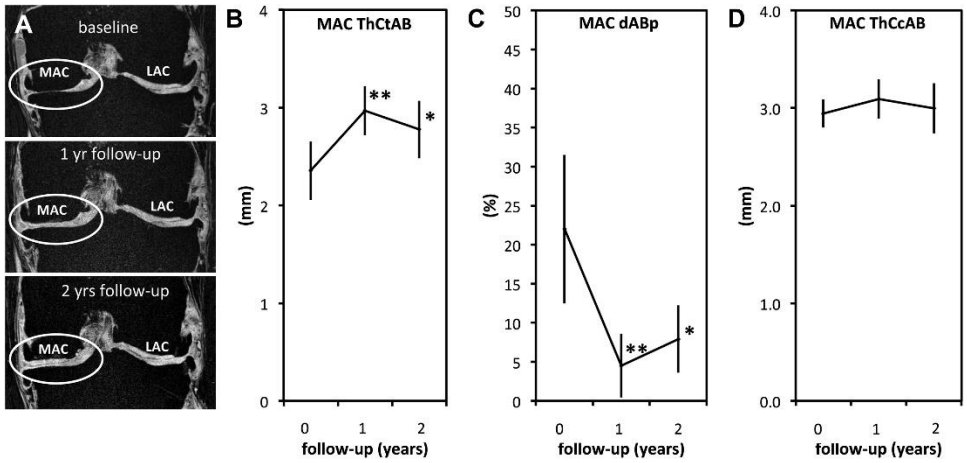

Figure 2.3: Physiological and radiological trends in cartilage thickness following KJD, reprinted with permission[5]

Five-year follow-up to this pilot study still showed positive effects from KJD, although trends through this timeframe continued towards decline[5]. In fact, three of the original cohort of twenty participants had total knee replacements in this time due to declines from OA. However, WOMAC and VAS pain and function scores were still improved from baseline. Similarly, the minimum JSW in the distracted knee was still higher than at baseline, although the most affected compartment JSW had returned to baseline levels.

The results of this pilot study point to a new direction for OA research. Unfortunately, the pilot study saw serious complications due to the surgical fixators that will limit the widespread application of this technique. Specifically, two participants in the pilot study had pulmonary emobli because of open pin tracts, and almost all (n=17) are reported to have needed antibiotics to treat pin tract infections[3]. These complications pose serious limitations on future widespread testing of KJD as a method for treating OA, as larger cohorts increase the number of harmed individuals.

To further study the benefits of long-term KJD, a method for providing distraction load is required that does not require an open wound tract. Ideally such a method would not require

surgical intervention at all. The method proposed to overcome this challenge is a knee brace that can apply distraction loads, providing a long-term method for applying force without surgery.

2.3 Osteoarthritis knee braces

Knee braces are orthotic devices that are designed to apply mechanical load to the leg for support or correcting alignment. Knee braces for treating OA typically try to correct varus/valgus moments and malalignments[15]. This countermoment is usually created through a narrow rigid frame or nylon surface, applying opposing coupled forces at three or four points along the leg. An example of such a knee brace is shown below:

Figure 2.4: Left: An example of a knee brace, reused with permission16. Right: A diagram showing the moment-generating loads applied by a knee brace

The knee braces presently available in the market are made from aluminum or magnesium alloys, carbon fibre and rigid plastic, or flexible nylon. These knee braces apply their forces with one or two arms running along the leg with connecting bars, which are coupled with straps to hold the brace on the leg. Because the forces are applied across the leg as concentrated loads (rather than being distributed across broader components), there are few braces that cover much of the leg – their designs are highly optimized for creating varus/valgus moments and little else. This method of loading seeks to treat the symptoms of OA (pain, stiffness, and malalignment)

with no other physiological effects. There is, however, existing controversy concerning their effectiveness.

The OARSI guidelines on the treatment of osteoarthritis summarize the controversy around OA knee braces as part of their review of biomechanical interventions in general – they recommend these devices as prescribed by specialists but acknowledge reviews that describe the evidence for their effectiveness as "limited due to heterogeneity and poor quality of the available evidence"[2]. The review in question was published by Duivenvoorden et al.[17], which assessed clinical trials involving knee brace effectiveness at reducing pain and improving function. Duivenvoorden et al.'s review presents a dissenting voice compared to other reviewers, most of whom agree that knee braces at least succeed in reducing pain[18-20]. This difference may arise from the constraint of clinical trials in the Duivenvoorden review – the reviews by Steadmann et al.[18], Petersen et al.[19] and Maleki et al.[20] did not have this constraint and included observational and pilot studies.

Even with dissent among reviewers, there is evidence towards knee braces reducing OA pain. Summarized by Moyer et al. in their review[21], many studies find that knee braces improve WOMAC scores for pain[22-27]. Interestingly, Draganich et al.[28] compared off-the-shelf knee braces to custom braces and found that while both groups improved pain scores, custom knee braces helped restore function where off-the-shelf braces did not. This suggests that custom knee braces interact more effectively with the body.

The crux of the controversy around knee brace effectiveness is biomechanical rather than clinical. This controversy is best summarized by Steadman et al.'s review[18], which focusses on a number of biomechanical measures of gait such as external knee adduction moment (EKAM), walking speed, self-selected walking parameters, and (in some cases) knee JSW. In general, unloader knee braces appear to reduce EKAM[26,27,29-31] with some caveats. Again, Draganich's study found that the custom knee braces successfully reduced EKAM where the off-the-shelf braces did not[28]. Factors such as pairing with insoles[24] and initial direction of malalignment[16] may also influence reductions in EKAM. In contrast, Hart et al.'s study suggests that the load applied to a brace does not affect whether or not a knee brace may reduce adduction moments[32]. The variety of findings and range of factors raises concerns regarding the compatibility of knee braces with individual cases. The research reported in this thesis was performed under the belief that the inability of knee braces to have consistent biomechanical effects is partly rooted in the

indirect method of loading – countermoments do not directly oppose the forces passing through the knee joint but rather shift their location. Inter-personal variability add even more variability to this indirect mechanical approach.

The evidence surrounding OA knee braces in the literature shows symptomatic relief without the physiological or gait changes required to delay OA progression. The disparity in these results can be directly compared to the distraction enforced in the KJD pilot study. Some knee brace studies have found changes in alignment[24,32] including one that used three-dimensional (3D) fluoroscopy[33]. Contrastingly, fluroscopic results found that this alignment change could open the most-affected-condyle but was inconsistent across brace design and participants. Another study using biplane radiographs found similarly inconsistent results[25].

Varying results across different designs speak to a mechanical problem rooted in the operating principle itself. The loads required for an unloader knee brace to pry open a collapsed knee compartment are extremely high; too high for the narrowness of the frame of current knee braces to distribute into the leg, It may be more effective to directly oppose the loads passing through the knee and pull the bones apart, as provided by surgical fixators, than to rely on a moment to open one compartment of the knee indirectly. The difference between these two loading schemes is illustrated in Figure 2.5.

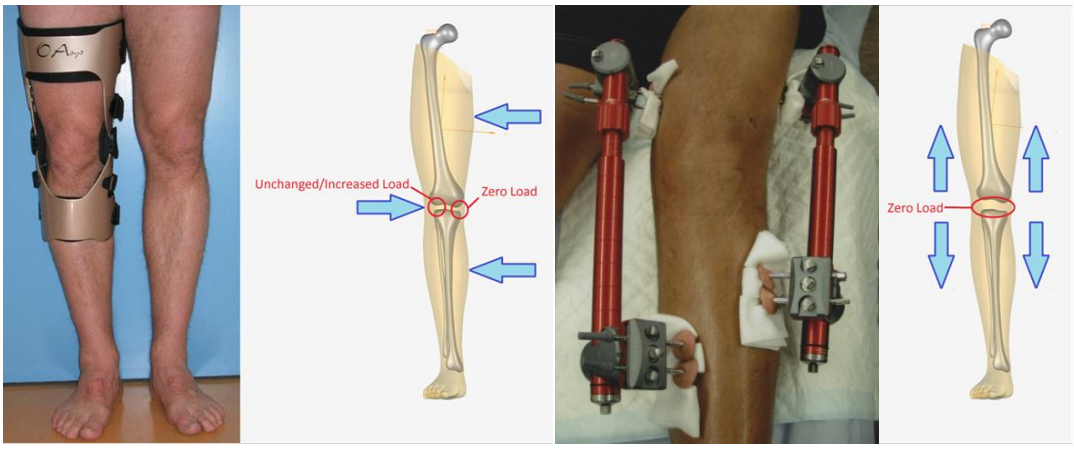

Figure 2.5: Comparisons of the traction and moment loads applied by knee braces[16] and surgical devices[5]

To achieve the desired transformation in loading, a change to knee brace interfaces (the components of the knee brace that contact the body) is required. This change necessitates study of the interface forces and their distribution across the leg surface.

2.4 Modelling of Biomechanical Interfaces

Biomechanical interfaces are challenging to quantify through both empirical measurements and modelling. However, the results of these investigations can provide detailed models which can be used in design and optimization of knee braces for desired applications. Pierrat et al. have developed one such model using CT images and non-linear tissue models to create a FE model that could then be employed in parametric optimization of a knee brace. The authors were able to study the effect of parameters such as brace stiffness, length, and coefficient of friction at the brace interface on stress at the tissue surface[34]. An example colour map of their simulation illustrating the model's ability to predict these interface stresses is depicted in Figure 2.6.

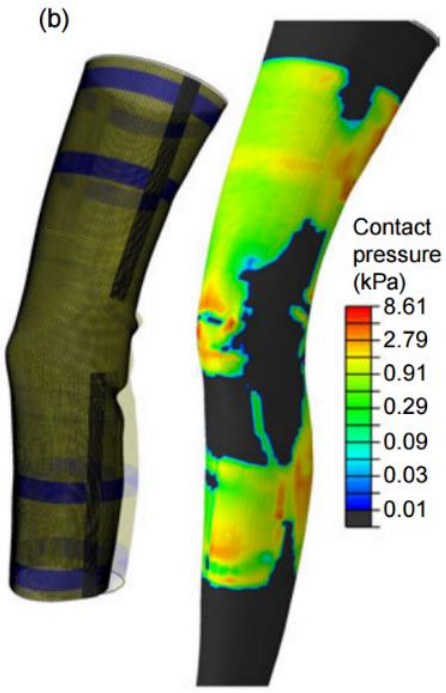

Figure 2.6: Example of an interface model, reproduced with permission[34]

A similar model would be an asset in designing an OA traction knee brace but these models require validation. Considerable work has been done for similar studies of lower leg prosthetics (which create traction loads similar to the desired effects of KJD), evolving towards dynamic,

validated models[35]. Flexible pressure sensors have been designed and tested for measuring prosthetic socket interfaces[36,37]. These sensors are designed to measure forces normal to the surface and have well-known limitations in combined loading such as buckling, folding, and shear biasing in output voltages. Ideally more complicated systems such as Fibre Bragg Gratings[38] can be used to provide 3D dynamic data. However, given the scarcity of data, there is still significant clinical relevance to simple pressure measurements given that they can be related to comfort and overall effectiveness[35].

There have been attempts to relate indenter pressures on the residual limb to a model to determine goodness of fit[35,39,40]. These models employ subject-specific imaging to develop models that accurately capture differences in geometry between subject's bodies. However, while these models relate interface stresses to the pain pressure threshold of the wearer, they do not validate these relationships with an overall pain score or interface sensor data. For a biomechanical interface such as a knee brace or prosthetic socket, the relationship between interface force and the comfort of the wearer are important areas for future investigation.

2.5 Summary

OA is a widespread musculoskeletal disease that affects tissues in the joints, causing pain, stiffness, and loss of function. A new method for combating the degeneration of these tissues in the knee may be long-term joint distraction, in which the joint is separated by a fixed distance for a number of months. This procedure has demonstrated the possibility for cartilage and subchondral bone to recover but has major complications due to the requirement for an open pin tract to externally fixate the bones.

The proposed method for overcoming the challenges of KJD is to instead employ a knee brace to apply distraction load, removing the need for surgery to distract the knee. Current knee braces employed in the treatment of OA use coupled forces to create moments about the knee to unload one compartment of the knee. These knee braces are effective at relieving pain but have not shown that they can apply the forces required to fully distract the knee. The problems with knee brace effectiveness necessitate a change in their design as they are constructed using frames that cannot apply the required traction forces. Further study of the biomechanical interface of such a high-load device is required.

Biomechanical interfaces are often investigated using FE models with experimental validation. It has been shown that such a model may be used to optimize soft brace designs, so there is potential to use interface information to optimize a high-load brace. However, the closest analogies to a KJD knee brace that are studied in this manner are prosthetic socket interfaces. In addition to FE models, flexible pressure sensors can be used to investigate the stress-state and forces at the boundary between the socket and residual limb. These methods may be replicated to analyze this boundary in a KJD knee brace and, ideally, relate the mechanical performance of such a brace to the comfort of the wearer. The current design paradigm of OA knee braces may be shifted to apply traction load rather than cross-loading to apply varus/valgus moments, allowing large-scale investigation into the promise of KJD as a conservative treatment of osteoarthritis.

3 Research Questions and Objectives

3.1 Research Question

The proposed research will investigate the design of a lower-leg knee brace and its interactions with the human body. The overall research question is: can a rigid knee brace be used to apply traction load to the lower leg? Further, the proposed research will investigate relationships between distraction load and wearer discomfort, and attempt to relate these factors to the mechanical interface between the brace and wearer's leg.

3.2 Objectives

To address the research question, the following objectives will be pursued:

1. To design lower-leg knee braces that can apply traction load to the knee; and
2. To test prototype lower-leg knee brace components and relate the traction load to wearer discomfort and interface force.

3.3 Hypotheses

For the design process prescribed in Objective 1, the hypothesis was that the artefact or system proposed (the lower-leg knee brace) would succeed in its purpose (to apply traction load to the knee).

The hypotheses for the pilot test described in Chapter 5 were determined during the design phase. We hypothesized that the longest knee brace design would have the lowest interface forces and, as a result, the lowest reported discomfort by study participants. We hypothesized that a “mixed” brace design comprised of short and long halves would have intermediate discomfort scores, and the shortest design the highest discomfort scores (with accompanying increases in interface forces).

Repeated brace failure for one participant prompted investigation of the relationships among leg shape, interface forces, and wearer discomfort. This investigation is described in Chapter 7. It was hypothesized that leg shape would correlate to measurements taken during the pilot study. Specifically, we hypothesized that increases in leg size and shape complexity (curvature) would reduce interface forces and wearer discomfort ratings.

3.4 Scope

Chapter 4 describes the design of the lower leg knee brace using planar FE modelling to determine different brace shapes to be tested. Chapter 5 describes the testing method that was developed to perform a pilot study on the prototype braces. This method was employed on a small cohort of 9 participants. The data from this pilot test was analyzed to for the relationships from Objective 2. Chapter 5 also describes the results of this analysis in terms of statistics and graphical relationships. In Chapter 6, post-hoc geometric analysis is used to relate participant leg shape to outcomes from Chapter 5. Chapter 7 discusses these results in the context of existing research. Chapter 8 concludes the research, addressing the limitations and future work arising from the pilot study.

4 Design Development

4.1 Introduction

The purpose of the design process was to create a new knee brace that delivers traction loading to the knee through the lower leg. These loads are of a large magnitude on a physiological scale (on the order of the wearer's bodyweight) but are relatively low compared to the strengths of engineering materials. The key issue in the design was then to distribute the load onto the body safely and comfortably. The distraction knee brace will need to be worn for long periods of time (up to two months to match the distraction period of the surgical pilot study). A prosthetic socket provides such a load and is usually worn for much longer than this time frame, but the force is directed proximally rather than distally. An effective design may then re-arrange a prosthetic socket to apply load in the opposite direction. By changing the orientation of the applied force and adjusting the area covered by the socket, this design has been adapted to the traction knee brace.

The design factors manipulated in this design were the area of coverage of the knee brace and the stiffness of the material. Area of coverage is a balancing act between avoiding sensitive areas while maximizing the area across which load can be distributed. Stiffness was determined by selecting the material for the knee brace. Investigation of the interaction between these factors began with a simple finite element model, leading to the iterative design of prototypes.

4.2 General Design Features

The proposed design employs high-coverage, prosthetic socket-like interfaces to apply traction to both the upper and lower leg. The initial concept for this design had nearly full coverage of the leg, with rigid connections to apply traction load at multiple points across the leg surface. A rapid-prototyping model of the design is demonstrated in Figure 4.1.

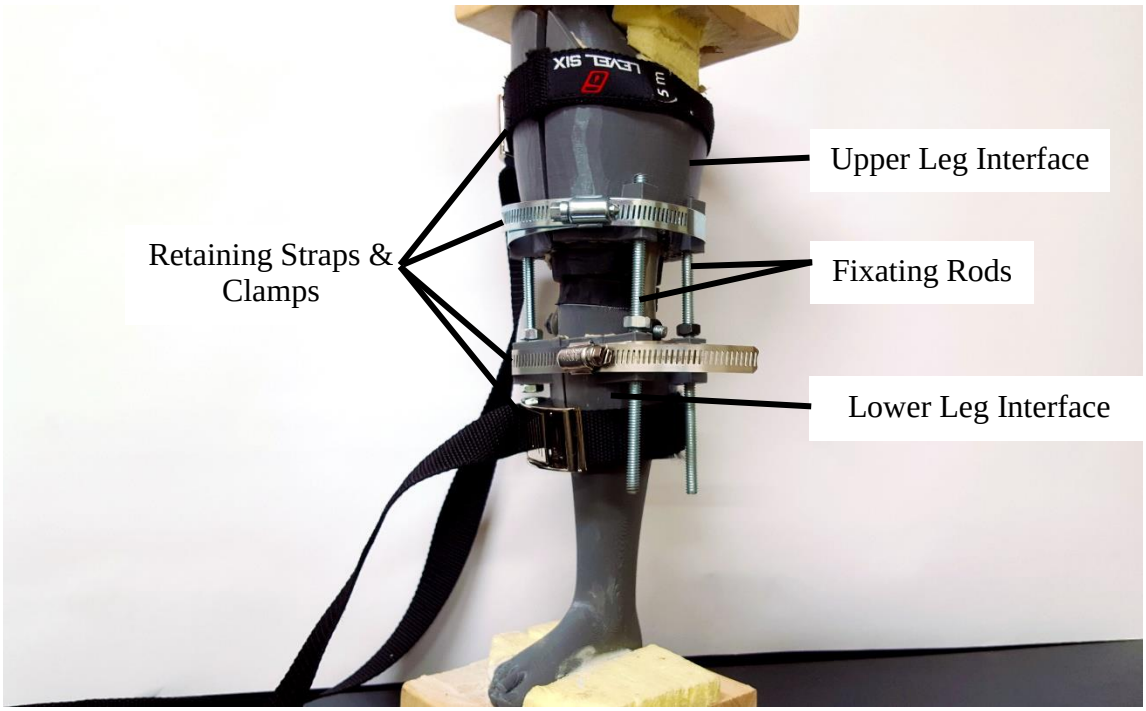

Figure 4.1: Model of a complete design concept

This design concept uses a simple mechanism (threaded rods) to apply traction load to the interfaces. At this stage of the design, straps (partially represented by hose clamps in Figure 4.1) apply preload to adhere the brace to the leg surface.

Early renditions of this design covered the entire surface of the thigh and the calf muscle. However, it was unknown if this was the ideal configuration for the design and, if the design were changed to cover more or less of the leg, what the comparative differences would be. The area covered by the brace became the primary factor to be manipulated while improving the design. The lower-leg interface was studied here due to the relative complexity of directing load away from the body.

4.3 Design Improvements

4.3.1 FE Analysis

4.3.1.1 Methods

A planar FE analysis of the lower leg was employed to observe the effects of changing brace area coverage on the brace-body interface. A simple shape was derived in ANSYS mechanical to simulate a generic lower leg (purple areas in Figures 4.2 and 4.3). Two rigid bodies representing

a knee brace (blue and red in Figures 4.2 and 4.3) were fitted directly to this body with a no-slip boundary condition at contact with the lower leg.

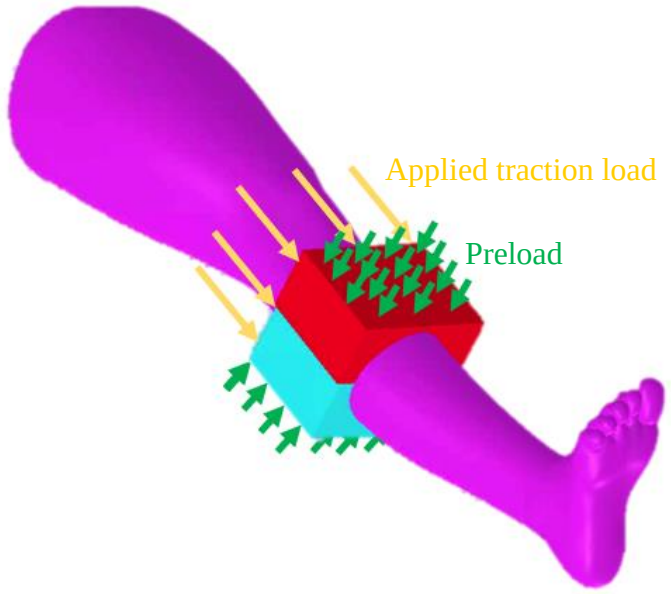

Figure 4.2: 3-dimensional representation of bodies used in FE simulation

All three bodies were modeled with 2-dimensional Plane42 elements representing the leg in the sagittal plane. Soft tissue was modelled with an elastic modulus of 13.8MPa and a Poisson's ratio of 0.475. These properties are considerably stiffer than 3D models for similar contact scenarios[41]. However, this tissue modulus allowed the models to converge without non-linear deformation. Without subject-specific data numerical results were only estimates for relative comparison of different lengths, so convergence of the model was prioritized. The elastic modulus of the brace material was 138MPa with a Poisson's ratio of 0.30. The properties for the brace material were analogous to a generic polyethylene thermoplastic[42]. This material model was selected to represent a common industrial plastic which is many times stiffer than the soft tissue.

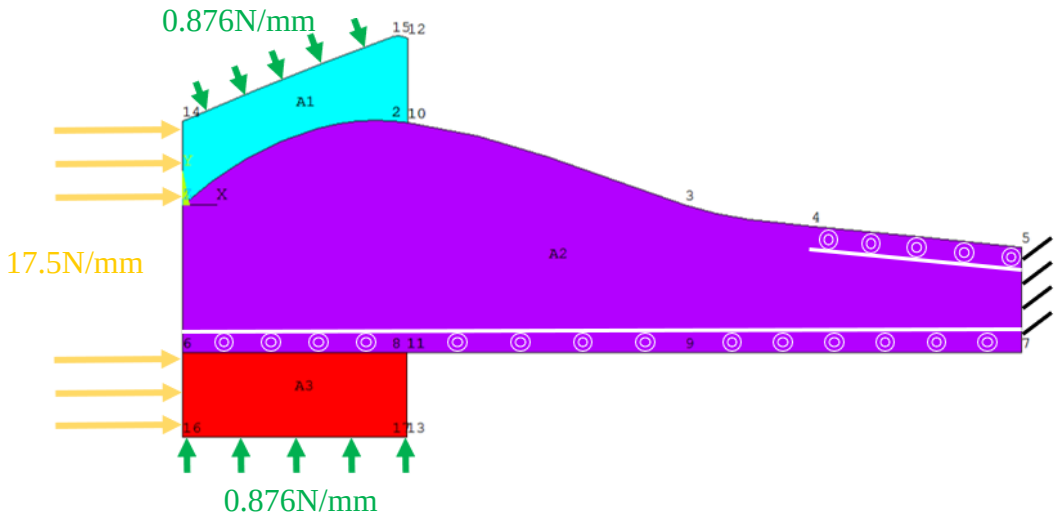

Figure 4.3: Boundaries and bodies in FE planar simulation of lower leg in the sagittal plane (colours of bodies match Figure 4.2)

Constraints were put on the planar FE model to simply simulate the bones and load applied to the brace. The vertical degree of freedom was restrained at the shin to simulate the tibia (the line between points 6, 8, 9 and 7 in Figure 4.3). The tangential degree of freedom was not restrained to allow for some skin-like movement at that surface. The distal edge of the body was fixed to act like a foot resting in place (against the ground or a wall) on the lines 7-5 and 5-4.

In this two-dimensional approximation, applied pressures were modelled as forces per length. A preload pressure of 0.876N/mm was applied to the exterior surfaces (line 16-13 and 14-12). A pressure of 17.5N/mm was applied to the proximal edge of each brace (lines 1-14 and 6-16). As the length of the knee brace was manipulated, the distraction force acting on the brace remained constant while the net preload increased (as a result of a constant distribution along the surface of the brace). This load case was solved for each brace configuration.

The effect of changing length was determined by resolving the load case for braces of increasing length. The percent of line segment 8-9 covered by the brace was the factor used to manipulate the length of each brace - braces were modeled for a coverage ratio of 0.05 to 0.99. Each brace had the same starting point (just below where the knee would be).

Von Mises stresses were contoured for all three bodies for comparison. Von Mises stress was selected as a stress measure to represent the net stress state in the leg. Any combination of compressive, tensile, and shear forces can affect comfort and the performance of the brace.

Visualizing the interface using von Mises stresses provided an overview of these combined effects. Maximum von Mises stresses and their locations were recorded for each configuration. Although units of MPa were recorded for von Mises stresses, these values could only be compared relative to each other due to the generic leg geometry and material models that were used.

4.3.1.2 Results

Von Mises contour plots were used to visualize the distribution of stresses along the brace-leg interface. Figure 4.4 demonstrates two of these contour plots. Plots for all lengths are given in Appendix A. Stresses were reported in default units of thousands of pounds per square inch (ksi) and converted into MPa. However, because this model used generic two-dimensional geometry with approximated material properties, the resulting values are only be interpreted comparatively within this study.

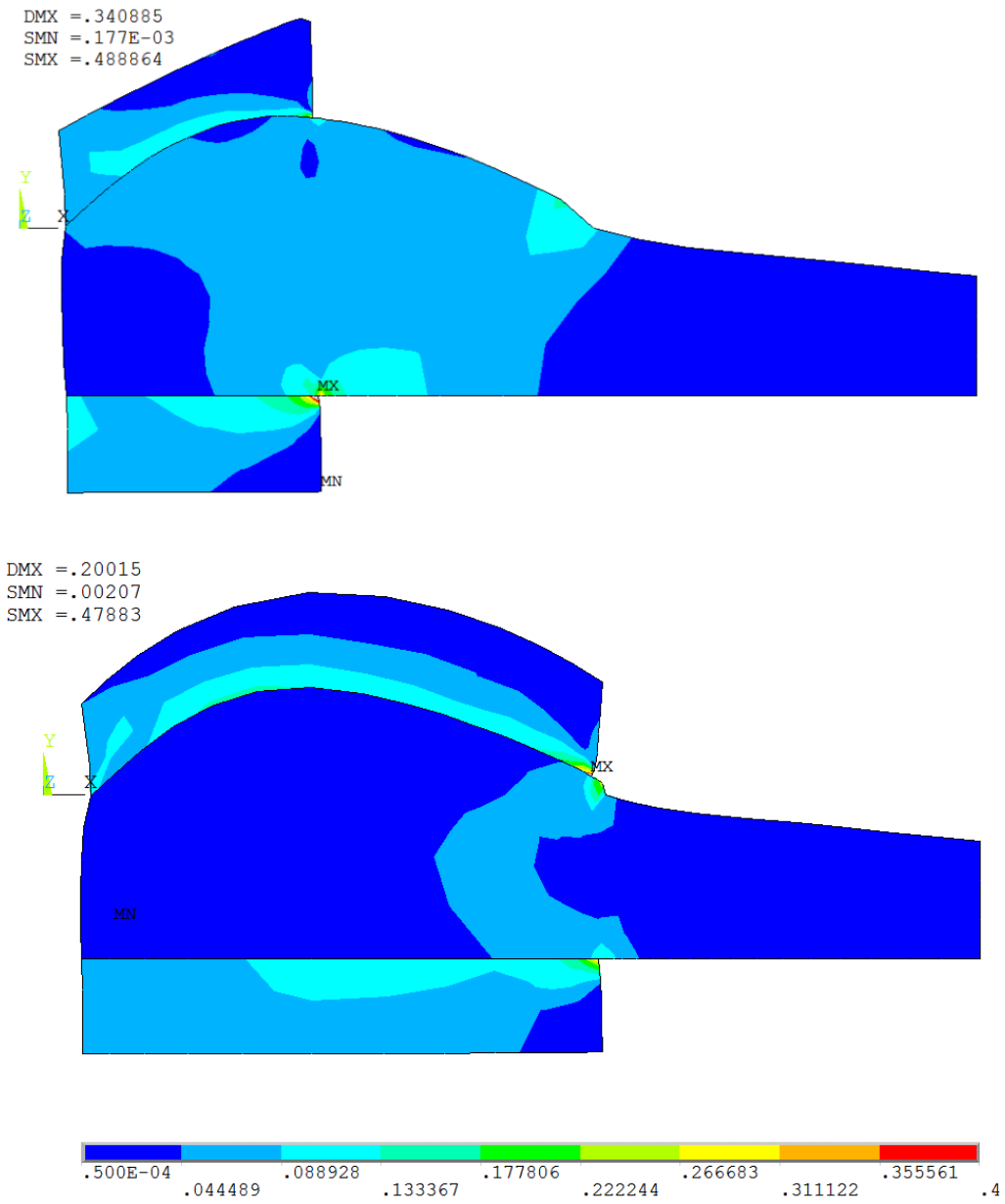

Figure 4.4: Contour colourmaps of von Mises stresses (shown in ksi) resulting from planar simulation. Two length ratios shown: 0.05 (top) and 0.99 (bottom)

Investigation with this model focussed primarily on the stresses in the leg directly immediately at and below the interface with the brace. The maximum von Mises stress and its location were recorded for each segment length.

Table 4.1: Summary of maximum von Mises Stresses in planar simulations, categorized by length ratio of lower-calf line coverage

% Segment Covered	Maximum σ_{VM} [Mpa]	Maximum Stress Location
5	1.87	Anterior Surface
10	1.80	Anterior Surface
20	1.14	Anterior Surface
30	1.14	Anterior Surface
40	0.996	Anterior Surface
50	0.862	Both anterior and posterior surfaces
75	1.02	Posterior Surface
80	1.11	Posterior Surface
99	1.48	Posterior Surface

4.3.2 Prototype Development

4.3.2.1 Methods

4.3.2.1.1 Design Model for Prototyping

Design of the prototypes began with a design space model to describe the relationship among concepts. A situated function-behaviour-principle-system-state (FBPSS) model[44] summarizes the requirements of a prototype knee brace. The FBPSS model was selected for the knee brace because it defines the design space in a way that is easily translated to numerical models (i.e. finite element models) and topographical and parametric optimization, all of which have already proven to be useful tools for studying mechanical interfaces. The FBPSS was applied to design a prototype brace for testing that could then be adapted into a complete knee brace with its own loading mechanism. This perspective on the design resulted in a design space that included additional functionality for quick changes to configuration and pressure measurement that may differ from or be excluded from a design space for a production knee brace.

Table 4.2: Summary of FBPSS Design Model

Model Component	Definition	Application to Knee Brace
Function	That which must be accomplished; the required transforms of energy and material	1) To sustain tensile load and transfer it to the human body 2) To be donned and removed by the wearer (with assistance)
System	The structure, boundaries, and components that define the design space	Minimum of two components: 1) Bounded by the shape of the wearer's body at contact surface 2) One boundary must have a fixed pattern to interface with other machinery
State	The quantities that define the system's way of existing; used in principle and behaviour equations.	1) Internal stresses/loads 2) Interface force (at human boundary) 3) Applied force (at standard boundary) 4) Geometry (brace coverage)
Principle	The chief concept that governs the system's performance	Static equilibrium of forces acting at the system boundary
Behaviour	Response of the system to stimulus (changes in state variables)	1) Distribution of forces at human interface 2) Deformation of the brace and human boundary

This model was an important tool for the comparison of different designs, and for interpreting the performance of different configurations of the same design during testing.

4.3.2.1.2 Design Iterations

4.3.2.1.2.1 Iteration 1 – Extruded Foam

The first prototype design that rose from the FBPSS model used extruded foam blocks as a building material. Blanks were machined from this foam to a common pattern that fit between the jaws of a testing system with an accommodating bolt pattern. The radius of the blocks was such that the interior could be machined to fit a wearer's leg. Changes in brace length were accomplished by stacking and bolting together sections of foam. An off-the-shelf drawer liner was used to pad the interior of these braces and provide higher coefficients of friction against the wearer's skin.

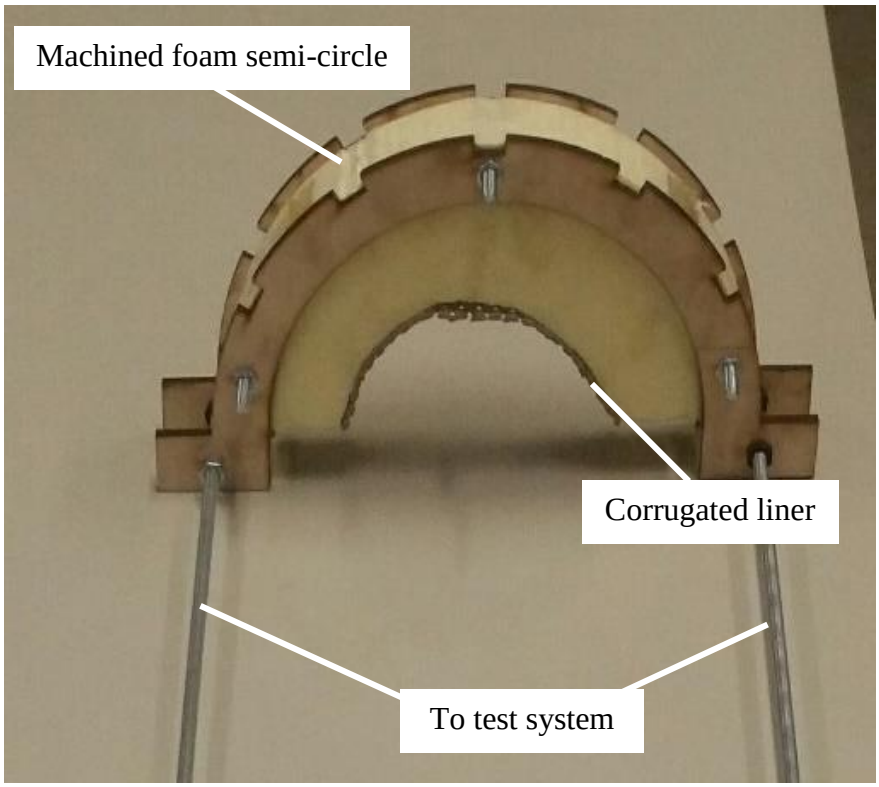

Figure 4.5: Prototype foam knee brace

The primary shortcoming of this design was in the expense required for customizing the shape to the wearer's leg. Ideally, computer numerical control (CNC) machining would be used to remove material from the foam blanks but this process proved costly and difficult. Similarly, producing die for moulding the foam was expensive due to the size of the die required. In testing, hand-fabrication was effective but slow and required a model of the wearer's leg to be freely available for fitting. Additional problems with this design included destructive wear on the foam and

bulkiness. Further, the foam deformed with respect to the leg surface – in cross section (as shown in Figure 4.6) like a cantilever beam fixed at the leg surface. This change in direction caused misalignment of the forces applied at the edge of the brace.

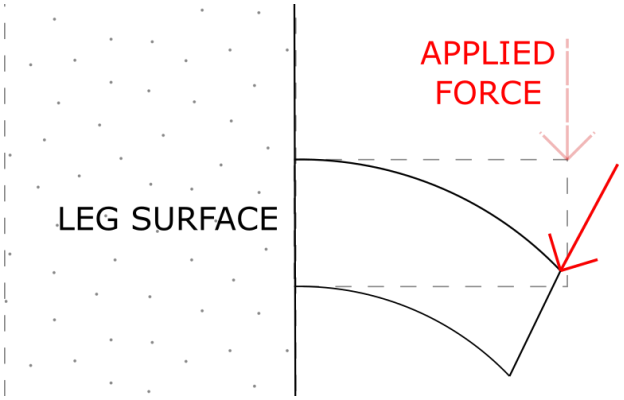

Figure 4.6: Foam knee brace loaded in cross section (undeformed and deformed shapes shown)

This deflection and destructive wear within the foam indicated that the foam designed was unable to sustain traction load (thereby failing to meet the function described in the FBPSS model). A stronger, stiffer material was required to achieve the balance of forces described in the FBPSS.

4.3.2.1.2.2 Moulded Fibreglass

Here a manufacturing process to fit fibre-reinforced polymers was selected. The first step in this process was to build a physical model of the wearer's leg. A plaster bandage was used to capture the shape of the lower leg, starting just below the patellar tendon and extending to the distal surface of the gastrocnemius muscle body.

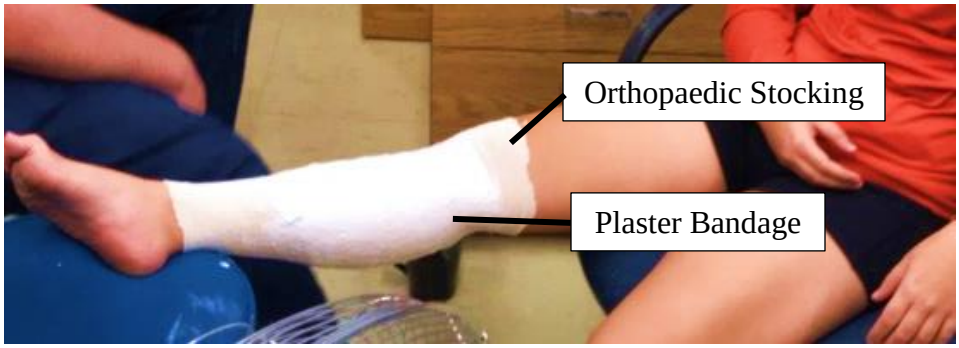

Figure 4.7: Plaster cast on participant's leg

This bandage, once solidified, was cut along the posterior line of the leg and removed. The bandage was then stabilized with polyurethane before being taped to a base and sealed with tape to form a mould. Moulds were sprayed with vegetable oil as a parting agent before plaster was poured in. Once set, models were scarified and smoothed with additional plaster as necessary. Care was taken during this process to preserve the shape of the leg – only blemishes resulting from the casting process were removed.

The next step in building a knee brace from this mould was to wrap the material around the plaster model. For a prosthetic socket, this process is simplified because the limb being fitted terminates – a full sheet of the socket material can be wrapped over the end and trimmed to create a manifold. This method was available (even though the limbs of the wearer extend, the mould itself terminates nearby) but the large amounts of material that would be fit and then cut away if we made the braces this way would be extremely wasteful. Delta-Lite Plus fibreglass casting bandages[45] were selected as a replacement material. Bandages were wrapped tightly around the leg model in a close approximation of the desired shape and then trimmed.

The advantages of the Delta-Lite Plus bandages extend beyond ease of manufacture. These bandages include a fibreglass substrate with a water-activated adhesive. It was observed that multiple layers of these bandages allowed the adhesive to consolidate into a visibly contiguous material. This property is highly desirable for the knee braces as it reduces the likelihood that layers will delaminate when fasteners and plates are held between the layers. Being able to hold on to fasteners is a requirement from the FBPSS design model, as is the rigidity and light weight of the material.

The final prototype design for testing arose from this manufacturing process. Complete Delta-Lite casts were made in two lengths, 3.5 inches and 7 inches. These lengths were selected to correspond (approximately) to the shortest length tested in our FE sensitivity study and the longest using the author's leg as the example. Parts from each cast were then able to be combined to create the third test design, with 7 inches of brace coverage on the shin and 3.5 inches on the posterior muscle bodies. This design was derived to observe the effect of increasing length on the anterior surface (hypothesized to reduce the interface force there) without the accompanying presence of the posterior brace to cause folding-over of the soft tissue.

The interior surface of each cast included orthopedic stockingette (to prevent the wearer's skin from contacting the fibreglass) and padded drawer liner to provide comfort and grip.

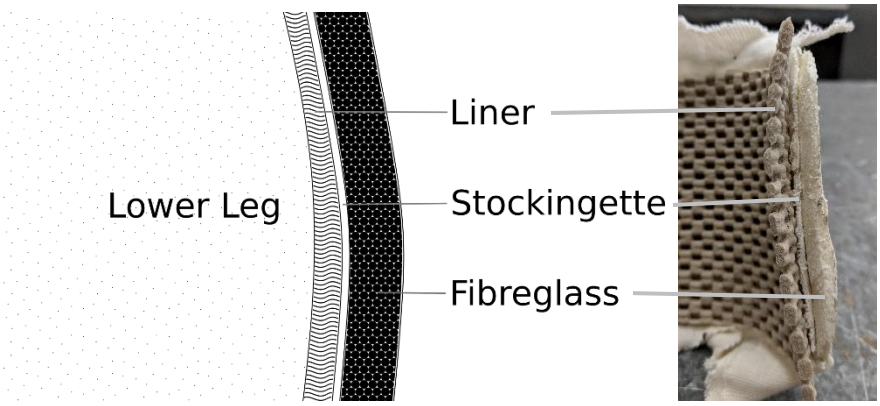

Figure 4.8: Section showing order of brace materials

Parting lines were required to fulfill the donning/doffing requirement from the FBPSS. These parts were placed to allow for testing of the load scenario described in our FE model. The parting line of the cast was made one the medial and lateral sides of the leg, leaving the solid brace in two halves (one posterior, one anterior). Early fittings indicated that a straight cut caused these the joint between these parts to pinch the skin, so a large chamfer was applied to the edge and the corners trimmed to reduce pinching and pain. These cuts made the brace surfaces over the tibia and gastrocnemius muscle body continuous, moving potential stress concentrations from the edge and providing a close analogy to the FE model in the sagittal plane.

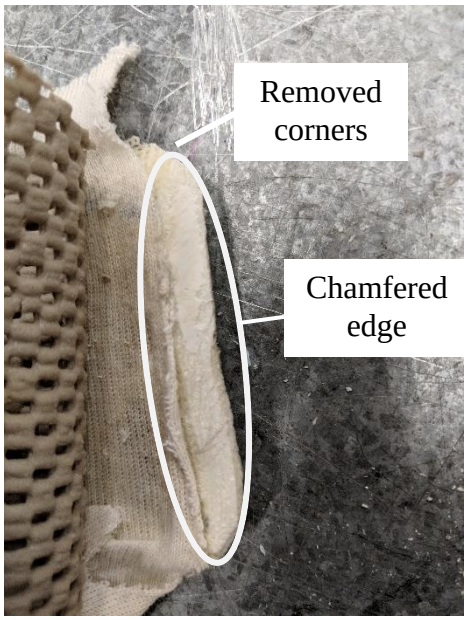

Figure 4.9: Edge and corner adjustments on fibreglass brace

Bolts were positioned in the centre of each brace half to act as the load transfer point with an external system. To maintain consistency in the bolt pattern, the bolts were held in place between two laser cut slates and glued in place. The plates and bolts were wrapped between layers of bandage as the brace was formed. The top edges of the plates were aligned with the proximal edge of the knee brace. The pocket of cast that formed around the fasteners was observed to be sufficiently stiff to transfer force into the surrounding brace.

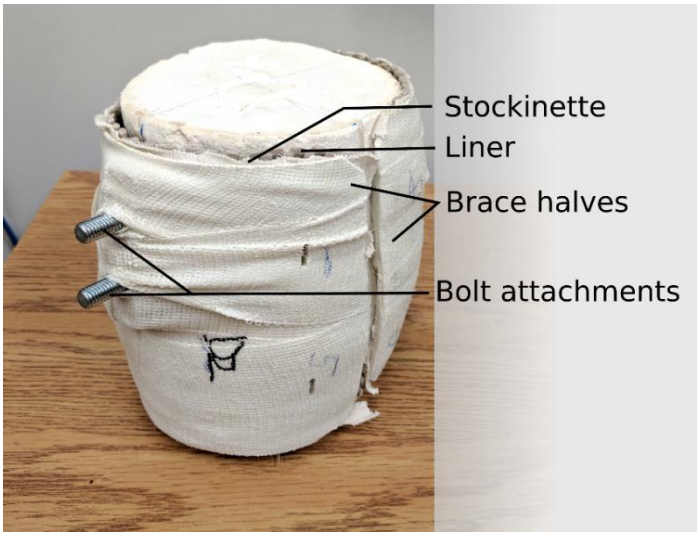

Figure 4.10: Completed prototype knee brace on plaster model leg

4.4 Discussion

4.4.1 FE Model

Planar elements were used to simulate a generic lower leg interacting with a rigid knee brace at a constant traction load. Up to 50% coverage of the lower calf line, maximum von Mises stresses at the brace interface reduced as brace length increased. These stresses were concentrated at the distal edge of the brace. This distribution pattern is likely the result of a moment created by the offset of the traction load from the surface of the leg, which also explains the reduction in stress at the distal end as the brace length increased. Beyond 50% coverage of the lower calf line, maximum von Mises stresses began to increase. Peak stresses initially occurred at the anterior surface of the leg, transferring to the posterior surface as the brace approached full coverage. It was observed that stress concentrations still occurred at the anterior surface of the leg – peak stresses in the posterior surface appeared to be the result of "folding-over" of the calf muscle (visible in Figure 4.4).

The results from this simple FE study also influenced understanding of how a rigid knee brace would function. Observed deformation and stress patterns indicated that the muscle body of the gastrocnemius (calf muscle) carried significant load and "pulled" along with the brace. In this case, the brace is pulling on the muscle body much in the way that physiotherapists would when applying traction with their hands. This pattern highlights the importance of the muscle body in carrying load although the peak stresses occurred over the tibia.

The conclusions of the FE analysis are limited because there is no validation for the quantities. It is well-established that there is a relationship between the surface pressure applied to a tissue and the pain felt, typically described as the Pressure Pain Threshold (PPT). These relationships are location-dependent and highly variable although lower stresses are generally more comfortable[43]. In this simulation, the different brace lengths can only be compared relative to each other and not in terms of an absolute estimate of wearer comfort. Despite this limitation, the patterns observed provided a hypothesis for physical testing. It was hypothesized that a longer brace would result in lower interface pressures and greater user comfort. This study also piqued interest in studying asymmetrical braces – that is, a brace that is longer in the front than it is in the back. It was hypothesized that such a brace may reduce the peak pressure felt by the wearer on the tibia while covering less skin overall (reducing concerns with ventilation, weight, and form factor).

However, it was hypothesized that an asymmetrical brace would compromise comfort for these benefits.

4.4.2 Prototype development

Prototype development indicated that the bandage-cast fibreglass prototype design satisfies the design model set out in the FBPSS. The two-piece design had strong components to transfer load into the body, meeting the functional requirement with sufficient stiffness and strength to balance the state. This design helped ensure customization to each wearer's body while maintaining a standard bolt pattern for attachment to a testing system. By combining brace halves of different lengths, this design method had potential to be used to test multiple brace configurations.

One important improvement made through iterative design of the knee brace was the addition of the friction liner to the cast fibreglass. Early prototypes were not able to sustain even low loads without slipping down the surface of the lower leg. The addition of this liner allows the brace to fixate on the leg, more closely approximating the idealized boundary conditions of the FE model.

The main limitation on this design is its dynamic fit – as a wearer moves, the muscle body will change shape. Future work on this design could be to provide splits or areas of thinner material with higher compliance that could flex with the body during gait. However, the first tests on this prototype were be static tests that do not include muscle flexion.

5 Lower Leg Brace Testing

5.1 Introduction

The purpose of this study was to fulfill Objective 2 and test a lower leg traction/distraction knee braces for effectiveness, measured in terms of wearer comfort and ability to bear load. The interface forces for these braces were also investigated. This chapter details a pilot test for measuring these factors in a small sample (n=7) of healthy participants with three brace lengths (3”, 7” and a mixed design). Braces were manufactured to match each participant's right leg, and were tested by applying load with a cable which pulled the lower leg away from the body.

5.2 Methods

5.2.1 Participants

Nine participants were initially recruited from among the graduate students and faculty of the Colleges of Engineering and Kinesiology at the University of Saskatchewan (aged 25 ± 6 years). Participants were required to be over the age of twenty to prevent damage to growth plates in the knee as load was applied. The only other criterion for exclusion was a history of knee injury or surgery within the previous 12 months. Of the 9 participants, 3 were female and 6 were male. These participants were recruited verbally at group meetings with the approval of the University of Saskatchewan Research Ethics Board.

Each participant had an initial appointment during which their leg shape was captured using a plaster cast (previously discussed in Chapter 4). Using a plaster model made using these casts, two sets of brace components were manufactured per participant. Brace lengths were standardized across participants – 3.5” (nominally known as the 3” brace for note-taking clarity) and 7”. These lengths corresponded approximately to length ratios of 0 and 1 (maximum and minimum length) from the FE simulation when fit to a sample leg. The mixed design was derived from these components.

5.2.2 Apparatus

The loading apparatus for this study was adapted from previous works in physiotherapy which provided traction load to OA patients. In the original study, a soft greave was placed around the patients' lower legs and was connected to a cable. The cable was passed through a pulley with weights suspended from the end to apply a continuous force to the leg[12]. This system was

selected to be adapted as it allowed the person being tested to sit or lie down in relative comfort while the load was applied.

The concept of using a cable in tension to pull the lower leg away from the body was adapted for this study with several adjustments. The soft greave was replaced with the knee brace being tested. As a result, the cable could not simply wrap around the leg. As such, a metal frame (shown in Figure 5.2) was built to connect the knee brace to the connecting cable.

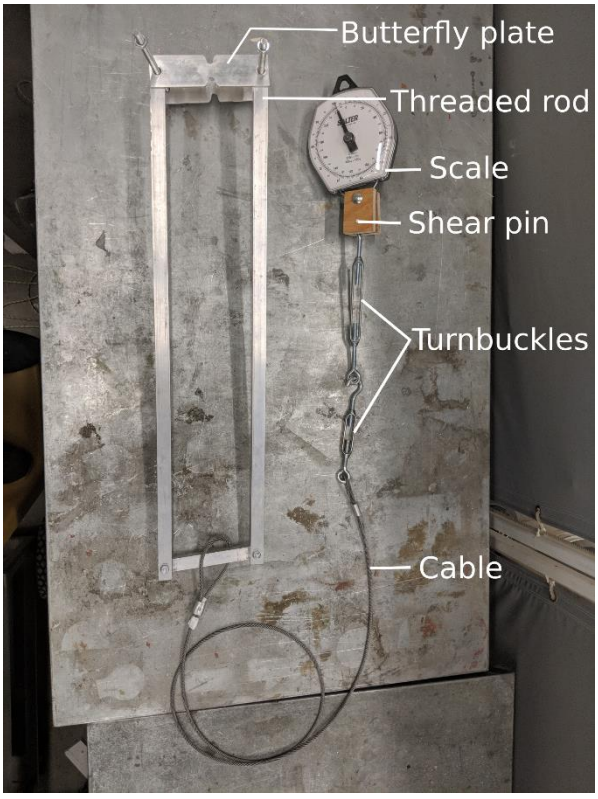

Figure 5.1: Frame and cable apparatus

This metal frame supported preload to the knee brace as it connected to the embedded bolts in the knee brace. Two threaded rods joined the butterfly plates with nuts that were tightened with the brace and wearer's leg inside, aligned by the two fasteners embedded in the brace. The compression of these two plates with the brace and leg in between provided the force that closed and compressed the brace, thereby adhering it to the leg. The rest of the frame was also connected to these rods, pivoting in place but supported by nuts that could be adjusted to ensure alignment with the midplane of the leg. The rest of the frame was composed of simple bars and

bolts. If the alignment of this bar with the participant's leg required the bars to realign, tape was used to gently hold the cable loop in place.

This study required increasing tension in the cable so an alternative to hanging weights was sought amid concerns that accidentally dropping weights could cause overloading (and thus injury) of the knee. To address this concern, the cable was attached to a turnbuckle which was then connected to a scale (to measure the applied force) and a fixed post. A shear pin was included at the connection between the cable and turnbuckle to release tension in case of an overload. A diagram of the apparatus is demonstrated in Figure 5.3. The tensile force was generated by shortening the turnbuckle, which pulled through the frame connected to the knee brace.

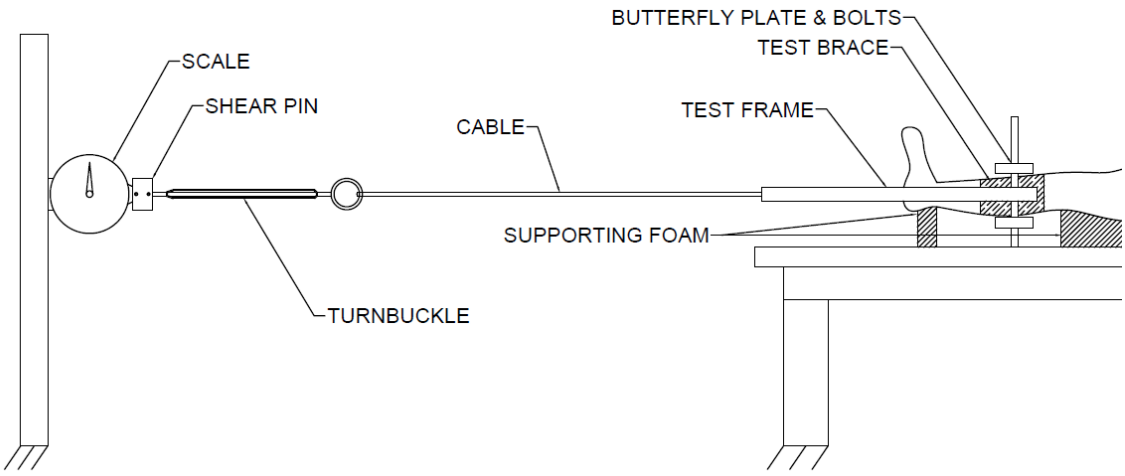

Figure 5.2: Arrangement of apparatus during test

5.2.2.1 Interface Force Sensors

Eight Tekscan FlexiForce A502 flexible force sensors were used to measure the forces between the knee brace surface and the participant's leg. These sensors were piezoelectric resistors that change impedance when strained. Changes in voltage as a result of this changing impedance were measured using a MCP6004 comparator operational amplifier. A comparison voltage of 0.125V and a feedback resistor of 1MΩ were used in this circuit to achieve the desired force sensitivity range.

The leg surface was divided into eight sectors, each with a sensor measuring the peak force over a $4in^2$ area within the sector. The surface of the leg was divided into quadrants by drawing two

lines, one through the apex of the shin blade and another normal to the first. These lines defined the quadrants. The surface covered by the 7" brace was then divided into proximal and distal halves, resulting in a total of eight sectors. Each sector was numbered as shown in the diagram below. Sensors were placed in the distal-proximal midpoint of each sector, ¼" offset from the anterior or posterior line.

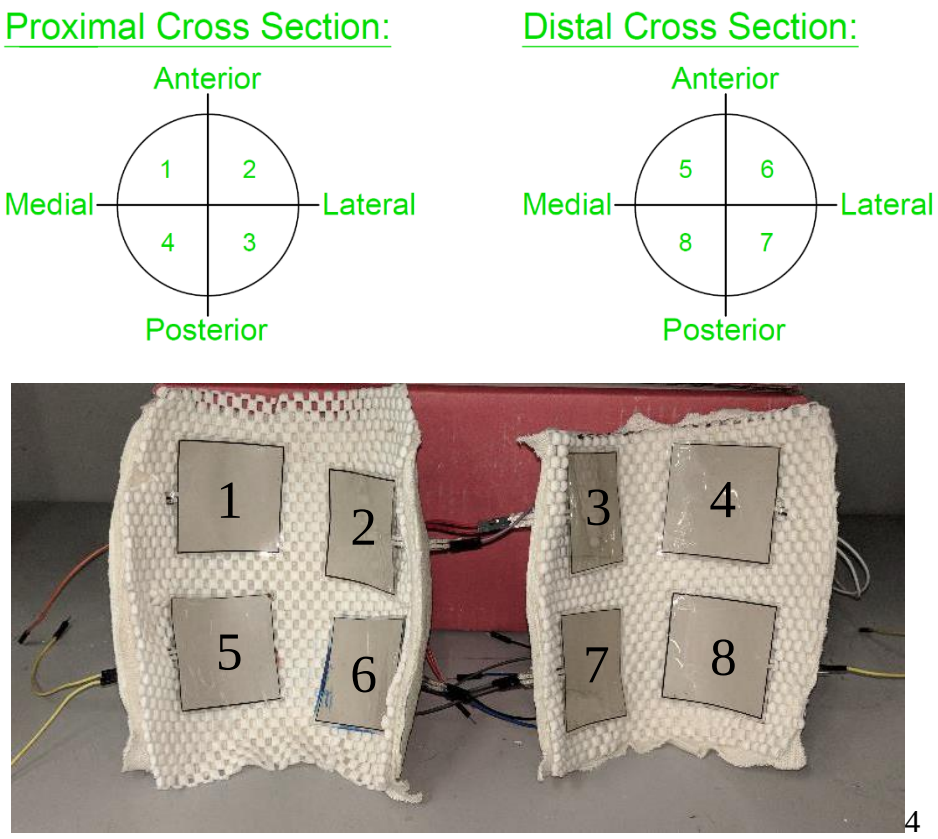

Figure 5.3: Division of brace area into measurement sectors, with sensors (numbered) mounted in a 7" brace prototype

Each sensor was individually conditioned and calibrated. Shear sensitivity is a well-documented concern when employing pressure sensors in biomechanical applications. However, previous tests have indicated that repeated shear loading of flexible sensors reduces their sensitivity to shear loads[46]. A Zwick linear actuator was used for calibration such that each sensor was individually exposed to a cyclic compressive load with an amplitude range of 10-100N for 10,000 cycles. This load was applied to the sensor with a 45-degree bit, resulting in a combination of compressive and shear loading across the sensor body.

Sensors were further conditioned with static loads as per manufacturer guidelines before every test. Each sensor was individually calibrated using the Tekscan procedure of applying static loads and fitting a curve to the resulting voltages. Calibration was performed on a curved foam insert with the same liner material as the braces to best approximate the intended application. Either a ratio of polynomials or power-law relationship was fitted to the response of an individual sensor to provide a relationship between output voltage and force.

5.2.3 Test Procedure

The following procedure was performed three times for each participant with three brace configurations (as shown below).

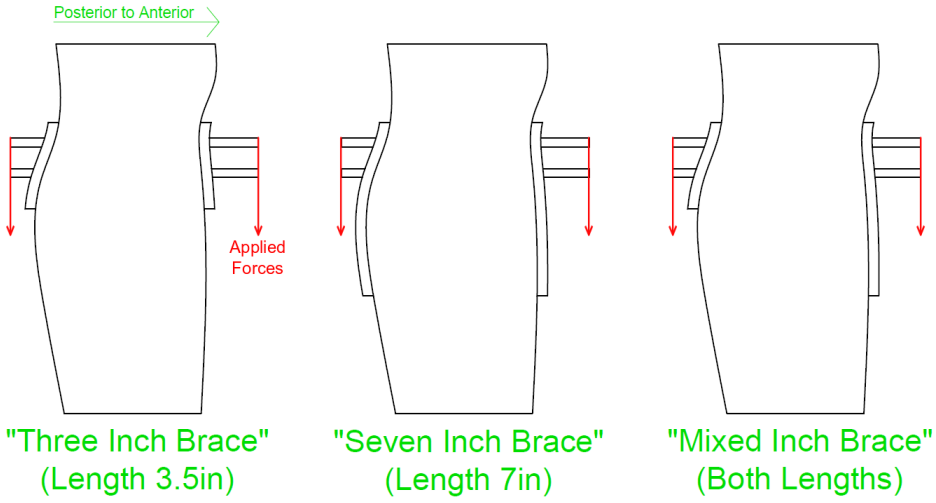

Figure 5.4: Three brace configurations for testing

Before each test, the brace components for the specific configuration were placed on the participant's leg outside the test frame and checked for fit. Slight modifications to the liner were made as required. Participants sat on a foam pad during each test with their right leg extended, using their left leg to brace themselves if required. The right knee was positioned with foam blocks and rollers to ensure that it was extended but relaxed. Participants were asked to keep their knee and toes upright but in a comfortable position, pointing their heels towards the post where the cable connected.

Once in position, the brace halves were connected to the butterfly plates of the test frame and positioned below the knee as demonstrated in Figure 5.2. The frame was tightened around the leg

until the brace was firm and the liner visibly compressed (typically until the nuts were hand-tight). If required for the longer braces, an additional strap was placed around the distal sectors of the brace to ensure full contact. The brace was considered fully closed when the joints of the brace were approximately in the manufactured position. With the brace in place, the first measurements were taken before the cable was connected and load applied.

Participants self-reported their discomfort verbally. An 11-point Likert scale from 0 to 10, also known as the Numerical Rating Scale (NRS), was used. Patients were instructed in the use of this scale, zero being no pain at all and 10 being the worst pain imaginable[47]; a rating of 2 corresponding to a skinned knee or stubbed toe; and a rating of 7 was determined to be greater pain than one would anticipate in their daily life (e.g. crushing a finger in a machine). At each load increment participants were asked to use this scale to report their discomfort while force readings were taken.

Electrical leads from each sensor passed through small holes in the brace, allowing the comparator circuit to be connected to each force sensor in turn. Leads were colour-coded to ensure measurements were related to the correct sensor. A Diligent Analog Discovery Module (ADM) and Waveforms software[48] were used to power the comparator circuit while simultaneously reading the voltage across the sensor. At each load increment, the oscilloscope channels of the ADM were connected to every set of leads and the cursor function was used to determine the output voltage, which was then recorded in a spreadsheet with the verbally-stated NRS score for that increment.

Both measurements (discomfort and interface force) were taken at the outset of the test. Once complete, the cable was connected to the turnbuckle and scale and force applied to the cable. Throughout the test, load was increased by closing the turnbuckle, increasing the tension in the cable in increments of $3kg_f$ (29.4N). However, the first non-zero increment of $3kg_f$ was not used as this little force was not large enough to suspend the cable and ensure distribution into the aluminum frame. Once the load was set, NRS and force sensor measurements were taken. The scale reading was observed intermittently during measurements to ensure that slight movements by the participant did not reduce the tension in the cable. As measurements were taken, participants were free to give qualitative feedback on their perception of the brace (the location

of pressure points, comfort of one brace relative to the other, etc.) which was also recorded. This process continued until a limit was reached that would end the test.

There were multiple conditions that could result in the end of a test. First, participants could choose to end the test at any point if they became too uncomfortable and did not wish to continue. Second, there were limits on how much force could be applied regardless of wearer discomfort. The first "soft" limit that was consistently striven for was one-third the participant's bodyweight. If this limit was reached and the participant wished to continue, the test would proceed until the applied force was equal to one-half their bodyweight. One-half was the maximum force that could be applied during the test. The third condition that would conclude the test was if the patient reported a NRS of 7, which was deemed too high for this pilot study. Finally, it was observed that some circulation loss may occur at high loads. If discolouration of the skin was visibly detected (as shown in Figure 5.5), the test was immediately concluded.

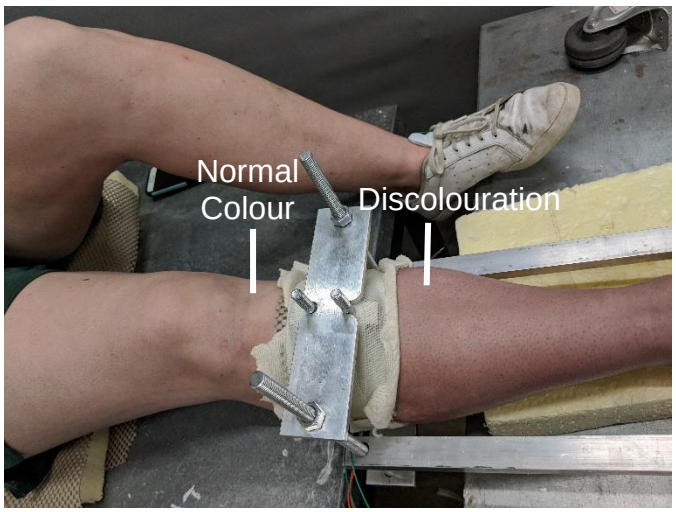

Figure 5.5: Example of discolouration due to loss of circulation

Once one of the end conditions was met, the force was released from the turnbuckle and the brace was removed from the participant's leg. Participants were encouraged to rise from the table and walk around the lab to restore circulation and relax their muscles between tests. A standard break length of 5 minutes was recommended to participants but they were encouraged to walk and stretch as long as necessary for the leg to feel normal. Once the participant was ready, the next test began.

5.2.4 Analysis

5.2.4.1 Self-Reported Pain

Patient-reported Numerical Rating Scale (NRS) scores for each brace were investigated using an analysis of covariance (ANCOVA) with a significance level of $p = 0.05$ via ISPSS statistics software. This analysis compared the pain scores among brace designs. Applied load (F) was included as a covariate affecting pain scores. This test assumed no interaction among the brace species and applied loads, i.e. regression lines drawn through all three populations on F-NRS plots are the same. This assumption was tested using the LMATRIX function in SPSS to run one-to-one comparisons of the slopes of each regression curve to each other.

5.2.4.2 Interface Force Profiles

Interface force measurements were grouped by brace species, applied load, and sector. Interface force profiles were plotted by sector for each load step. In these profiles, the load for each sector was averaged among participants and plotted as a radial bar with the other sectors.

The maximum interface force among all sectors of a brace was determined for every participant at every load step. This maximum interface force was compared to the self-reported pain for each load step. Pearson correlation coefficient was used to test for a relationship between maximum interface force and wearer-reported pain with a significance level of $p = 0.05$.

5.3 Results

5.3.1 Participant Inclusion

Of the nine healthy volunteers initially recruited for this study, one male participant withdrew due to a psychosomatic event (fainting) during the test. This event was reported to the University of Saskatchewan Research Ethics Board. After review, the Board approved continuation of this study.

One other male participated in all three tests but his data was excluded due to brace failure in two of his three tests. The mixed and 7-inch brace were tightened for this participant using the same criteria as the others, but the braces slipped off at low loads. This was attributed to a "smokestack-shaped" lower leg with little curvature. Attempts to tighten the braces any further were unattainable without alteration to the brace design, resulting in the exclusion of this

participant's sensor and pain data from the data set. This participant's results prompted the investigation of geometric parameters in Chapter 6.

The resulting data set consisted of pain and interface force data for seven participants (four males and three females). Two (2) of the participants gave low pain ratings on the numerical rating scale that were significantly different from the rest of the participants across brace species and load. These ratings were found to be outside the 95% confidence interval for each individual load with respect to the rest of the sample. These two data sets were thus excluded from the analysis of pain data but their interface force data, which did not differ significantly from the sample, were included for analysis. Also, one participant had four points in the mixed-brace test where the maximum interface forces observed were significant outliers. These points were omitted from interface force analyses.

5.3.2 Qualitative Feedback and Observations

Qualitative feedback during the tests was consistent. Most participants reported that their pain was focussed around the joints of the knee brace. This pain was unilaterally described as a pinching sensation resulting from the brace pieces pushing the skin together. In some cases, participants reported that they could feel both the traction of the brace on their skin and the pinching simultaneously and that the pinching was dominating their pain (resulting in higher scores). Many participants reported that the pinching sensation was worse at the corners of the brace halves, specifically in the proximal corners where the two halves meet.

Some evidence of load shifting to the distal edge of the brace was observed. Participants consistently reported the sensation that load was concentrated on the distal edges of the brace. At high loads, it was observed that a gap could form between the proximal edge of the brace and the participant's leg resulting from brace deformation. In these cases, contact was maintained over most of the leg surface. This effect was only visually observed in three participants.

5.3.3 Pain Responses to Differing Brace Designs

ANCOVA analysis of participants' self-reported pain, in relation to the applied traction load and controlling for the brace type, demonstrated differences in the performance of the different braces. Applied load was determined to be a significant covariate ($p < 0.001$) with a significant difference among brace types ($p<0.001$). Post-hoc examination revealed that the mixed brace design resulted in the lowest pain scores. Pain responses for the 3" brace averaged 1.2 NRS steps

higher than the mixed brace ($p < 0.001$). Pain responses for the 7" brace were slightly higher than the mixed brace, but not significantly different ($p = 0.349$). A plot of applied load vs pain can be found in Figure 5.9 for the different braces.

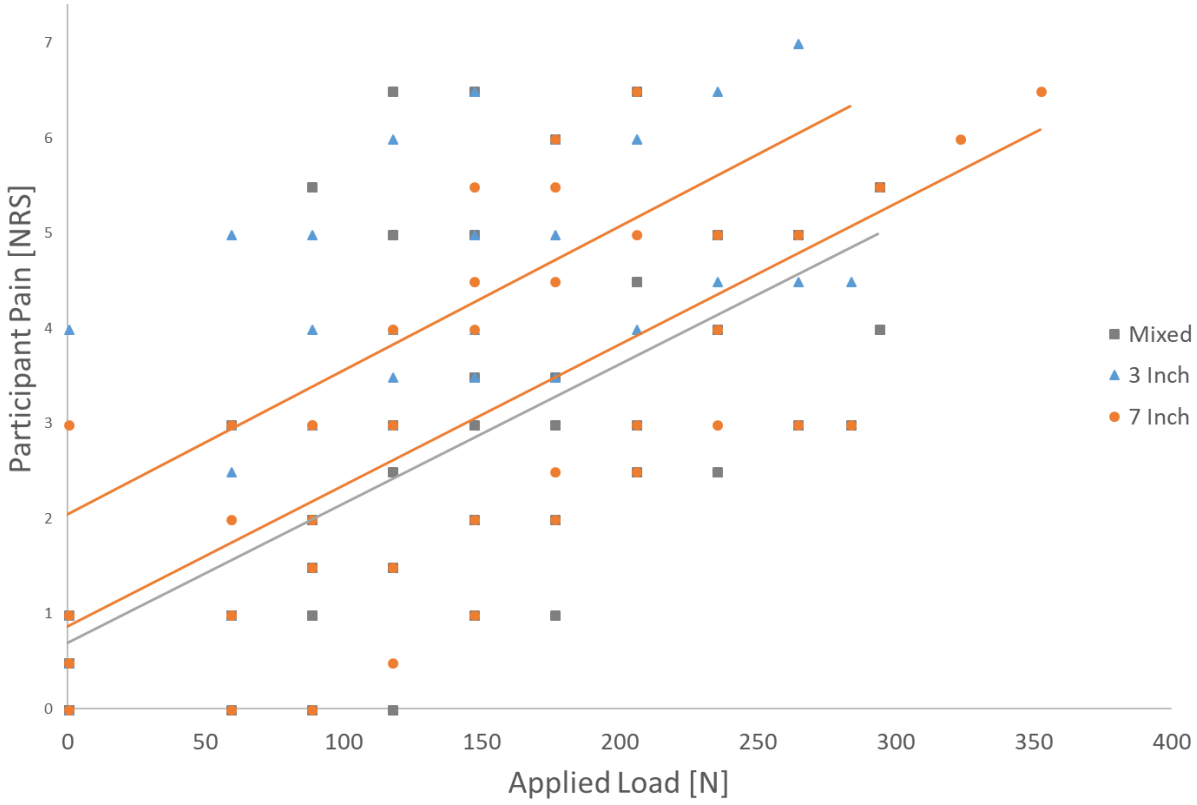

Figure 5.5.6: Regression model relating pain and applied load

In this full-factorial model, there was shown to be no interaction between the brace and applied load, which would have resulted in a difference in slope among regression lines. One-to-one analysis using the LMATRIX command confirmed this finding.

5.3.4 Interface Forces

Load profiles provide insight into differences in load distribution among the brace designs. The profiles for the baseline (zero load) point and two applied loads are given below.

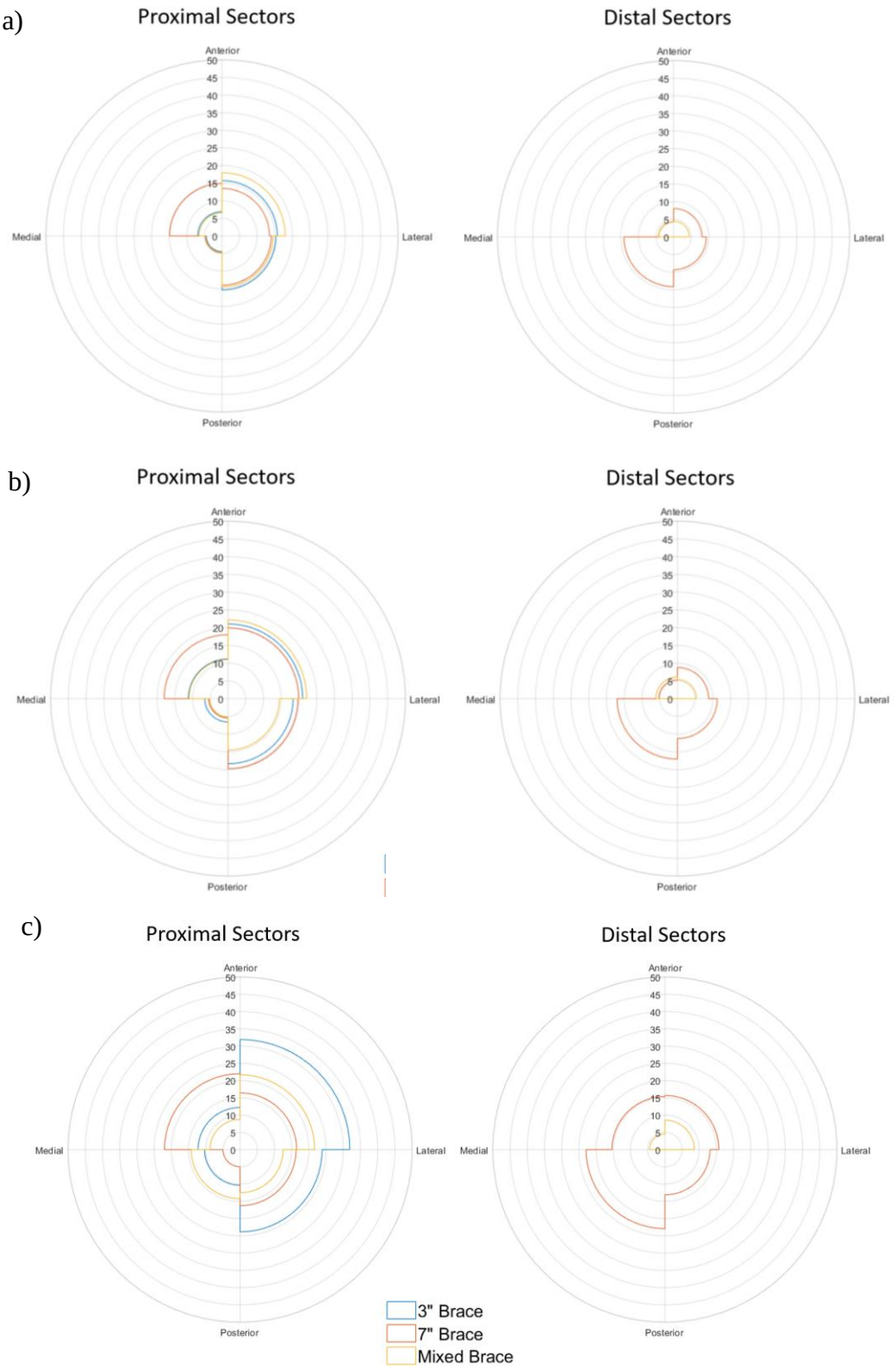

Figure 5.7: Average interface force profiles (in Newtons) a) at baseline; b) at 117N of applied load; and c) at 206N of applied load.

The baseline profile shows the average distribution of brace preload across the leg surface. The profile for the 3” brace exists only in the proximal sector because this brace did not exist in any of the distal sectors. Similarly, the profile does not exist for the mixed brace in the posterior sectors of the distal profile. The baseline profile was compared with those corresponding to 117N and 206N loads. The 117N profile is the highest profile with data from every test (all participants at all loads). The second profile for comparison to baseline was taken at a load of 206N, as this was the highest load for which there was a minimum of three readings for all sensors. Qualitative comparison of these profiles shows increases in all sectors of the 3” brace except the proximal-posterior-medial sector, which demonstrated a moderate increase overall. Increases in interface force were modest for the 7” and mixed designs. The 7” brace appears to carry more load in the distal sectors of the brace than the mixed brace.

Maximum interface forces for each load step were compared to self-reported pain across braces. A plot demonstrating the relationship between these variables is demonstrated in Figure 5.11. Each series has large variance in both pain and maximum interface force. No significant correlations were found between pain and maximum interface force for any of the three brace designs.

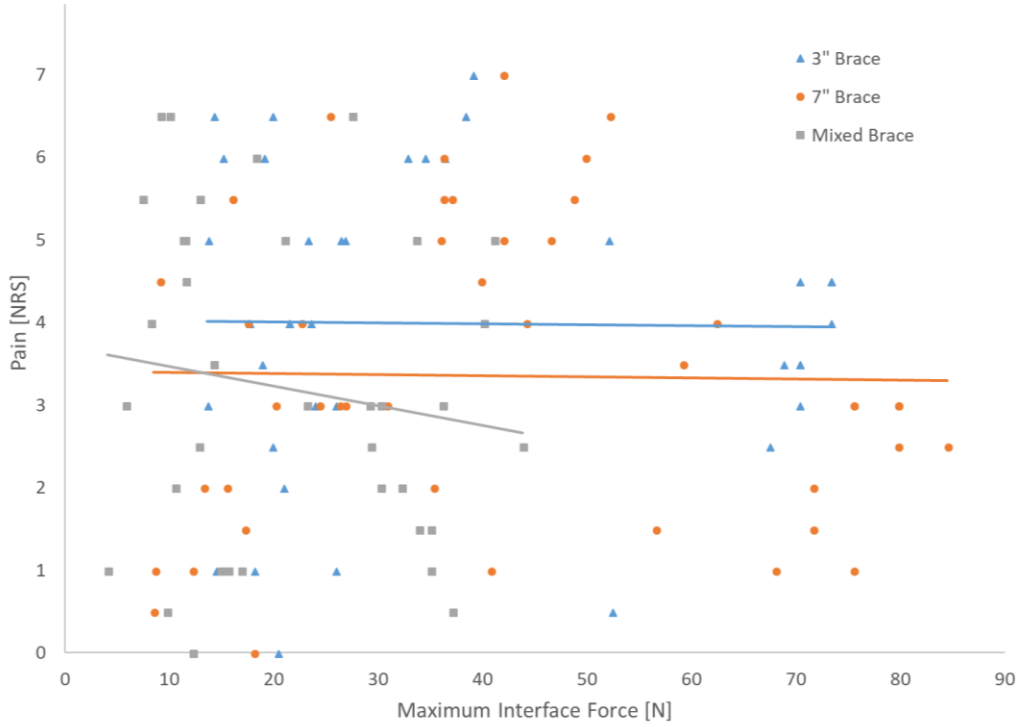

Figure 5.8: Self-reported pain and maximum interface forces for three brace designs

5.4 Discussion

The purpose of this study was to test the brace in terms of comfort and the ability to bear load. This study met this objective by showing that all participants were able to support 117N of applied load in all braces. Most participants were able exceed that load, with some reaching up to 300N of applied force.

The relationship between traction force applied to the brace and wearer discomfort was found to be brace-dependent. For the same applied load, the 3” brace had higher pain scores than the other two braces, indicating that it is the poorer of the three designs. The 7” and mixed brace did not differ from each other. Although there are variances to each data series, the rate at which applied load caused increased pain is the same across designs. Interface load profiles were developed for all sectors at 0lbf, 117N, and 206N of applied load. These profiles demonstrated an increase in force in the four sectors covered by the 3” brace. The 7” and mixed designs saw more moderate increases in force, but the 7” brace did demonstrate a shift in load towards the distal sectors. The

3” brace (the most uncomfortable) had large increases over few sectors, which would result in interface pressures approaching pressure pain thresholds and cause greater discomfort.

Qualitative feedback from participants during the tests both confirmed findings from the design phase of this study and provided new insight. The FE study described in Chapter 4 indicated a stress concentration for all braces at the distal edges of the brace. Some participants described feeling such a load concentration. However, the planar FE model could not predict the pain concentration at the joints of the brace.

The interface force profiles provided some insight into these differences. At 206N of applied force, the 3” brace carried larger loads in the proximal sectors than the 3” brace and the mixed brace, which could distribute load lower onto the leg. However, due to variance in sensor data, we were unable to detect a correlation between pain and maximum interface force.

Qualitative feedback from these tests suggests that different sensor locations may be required to correlate interface forces and wearer pain. Participants reported that their pain was localized around the edges of the brace. For this study, pressure sensors were located near the centre of each brace half. Qualitative feedback suggest that sensors are needed near the edges of the brace to measure the forces causing the perceived pain.

This study provides insight into factors that are important for the continued refinement of a rigid lower-leg knee brace for traction loading. The consistency across metrics where the 3" brace has higher interface forces and self-reported pain suggests that, if both are to be minimized, it is the worst design.

To achieve distraction of the knee joint that can be observed on radiographs, the forces passing through a knee brace will need to be greater than those applied in this pilot study. The relationships found in this study and the qualitative feedback suggest that the brace designers need to be cognizant of different ways of carrying load between the anterior and posterior surfaces of the lower leg. Designers should strive to maximize the area of the anterior surface of the lower leg that bears load, while being cognizant of the shape of the tissue on the posterior surface. Balancing these factors will allow the knee brace to bear load and generate traction comfortably.

One possible pathway to balance the design is to normalize the shape to the wearer's leg. In this study, fixed braces lengths were used across participants rather than assigning brace coverage based on the lower-leg length of each participant. This extra step in the customization process may allow future designers to better balance shape and size of the wearer's leg with the required distraction loads. Another possibility may be to normalize interface forces or pain responses to parameters such as leg length or use bodyweight – such analysis was omitted from this prospective study,

The primary limitation of this research is the size of the cohort for the pilot study. A small sample size and high variability in the interface force limited the statistical significance of the results. The resolution and location of the interface force scanning array was the other major limitation on this study. The sensule area of the Tekscan sensors in this pilot study was 4 square inches – sufficient to provide an idea of the distribution of force across the surface but attempts to divide the output force by this total area would result in a considerable overestimation of the pressure acting on that area. These sensors also did not cover the full area of the leg and did not provide enough resolution to directly observe the transfer of load to the edges of the brace. These sensors were, however, sufficient to show trends in the force distribution and differences among the braces when plotted as average profiles. Sector-by-sector analysis of the force data indicated these trends even if they did not reach statistical significance. In addition to the individual effects of leg geometry, preload on the knee braces was standardized by relative position of the brace and not the interface force measurements. Baseline differences in interface force may have introduced additional variance in interface force measures, but the baseline interface forces were not observed to differ greatly between participants during testing. This pilot study succeeded in meeting the general objectives of identifying trends despite these limitations, while providing a basis for more detailed study.

Sample size may have had an effect on the statistical significance of pain findings, in addition to the varying end conditions imposed to ensure participant safety. The ANCOVA analysis assumed that all pain scores were independent. In this study, each participant supplied a series of pain scores, meaning that each scores are in fact dependent. Another analysis, specifically a repeated measures ANOVA, could account for these within-subject effects. However, each participant's tests consisted of a different number of measurements depending on their

bodyweight and pain tolerance. A repeated measures ANOVA would require each participant to provide a pain score at the same number of points (potentially reaching above pain or bodyweight limitations).By assuming measurement independence, ANCOVA analysis allowed data series of different lengths to be considered for each brace design.

6 Geometric Analysis

6.1 Introduction

Conditions resulting in the exclusion of one participant indicated that the geometry of the lower leg may be an interesting factor for investigation. The factors chosen for analysis were the radius of curvature of the muscle body (as it was observed to carry significant load), the surface area of the leg in contact with the 3" brace, the volume of the section bounded by the 3" brace, and the maximum cross-sectional area of the leg. Curvature was analyzed in the sagittal plane as curvature in this plane would affect the shear-compression shift in surface forces that resist the applied load. Analysis of these parameters was performed using 3-dimensional STL files containing participant leg geometry obtained after the pilot test.

6.2 Methods

6.2.1 Digitizing Participant Leg Geometry

Point-cloud data was acquired with assistance from the computer modelling lab in the College of Archeology. Digital point clouds capturing the outside of brace models were captured using a NextEngine ScanStudio optical scanner and stitched together with the accompanying ScanStudio HD software (200DPI at 300 micron accuracy)[48]. Binary standard tessellation language (STL) files were made from these point clouds and were imported into GeoMagics Studio 14[49]. Geomagics Studio was used to smooth the surface and patch holes. The STL file was then remeshed with 2-mm triangles to enable export to MATLAB for analysis.

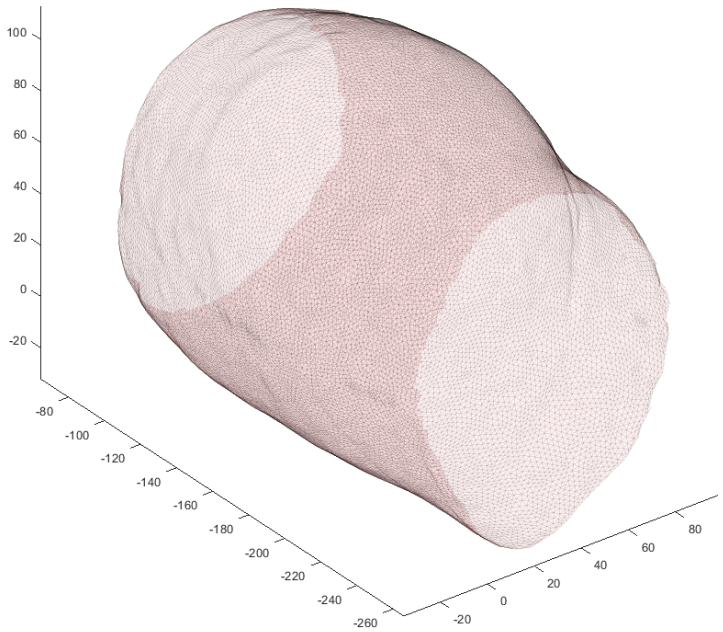

Figure 6.1: Example of a STL surface of a lower leg

6.2.2 Geometric Analysis

A custom MATLAB code was written with elements drawn from the Mathworks community that uses surface triangulation and intersection[50] to sweep from the distal edge to the proximal edge, searching for the greatest cross-sectional area (representing the widest point of the muscle body). The location of this maximum cross-sectional area was used as a basis for curvature analysis. Sections of the leg above this point were extracted from the complete scan, and another intersection taken (this time in the sagittal plane). The curved data representing the posterior side of the leg was then separated from the rest, and a circle fit using the Pratt algorithm for circle fitting[51]. The radius of the circle fit to these points represented the curvature of the extracted section.

Root mean square errors (RMSE) for each fit were calculated using the centre of the circle returned by the Pratt circle fit. Each point from the fit data set was assigned an error defined as difference between the fit radius and the Euclidian distance between the centre of the fit circle and the point as demonstrated in Figure 5.7. The total RMSE of the fit was determined using these errors.

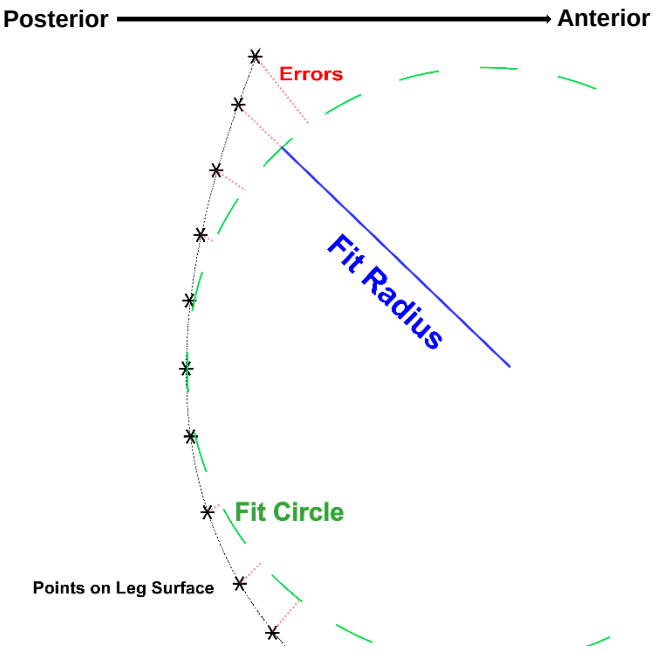

Figure 6.2: Sketch of error determination for Pratt fit circles

Circles were fit to a number of sections of increasing length for every participant. Section lengths began at 5 slices of 1mm (0.039in) long and increased in size by 2 slices (the distal edge of the fit section was maintained at the point of maximum cross-sectional area). The maximum number of slices tested was determined by the number of slices in the scan and the location of the maximum cross-sectional area. These fits resulted in many different curvatures for a single participant, so convergence criteria were developed that helped determine the actual curvature to use. These criteria were:

- A minimum section length of 35mm;
- RMSE values less than 0.25mm; and
- A section length that was 5-10mm smaller than a sudden increase in RMSE.

The convergence of each participant's series of fits was determined by examining plots of both RMSE and the fit radius (an example is shown below in Figure 5.8). Once a candidate section was determined, the fit was checked for outliers. The radii of curvature were then included as a factor in further analysis of data.

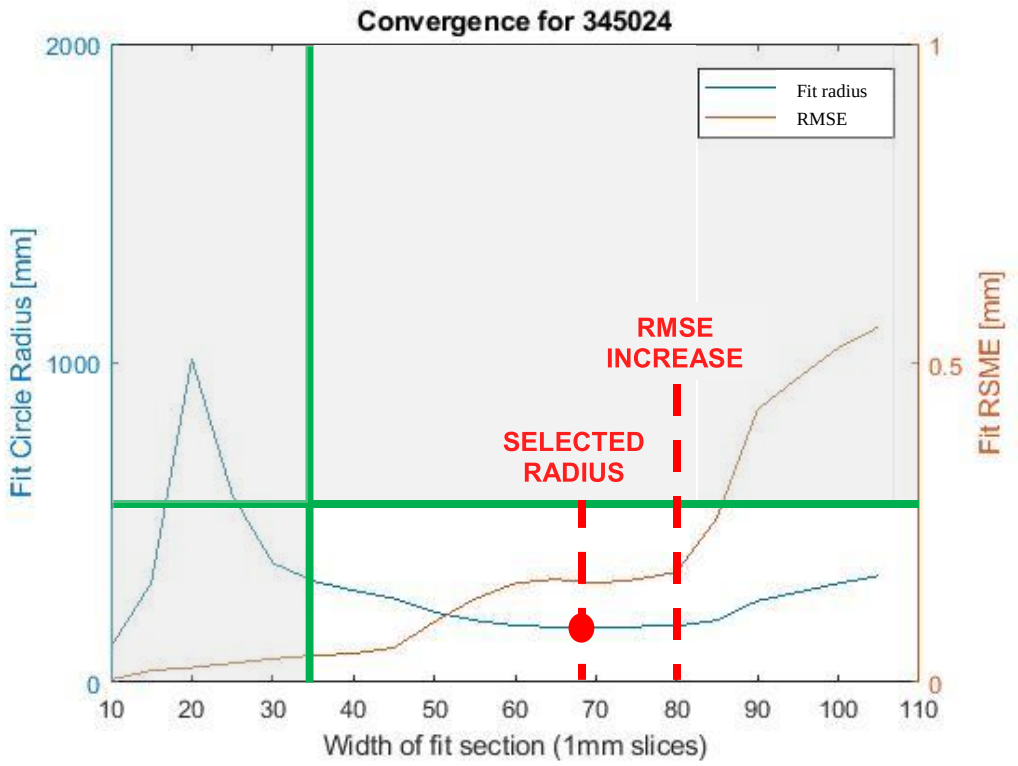

Figure 6.3: Example of a convergence plot for curvature fitting showing thresholds for fit width and RMSE (green and grey), the section width near a sudden RMSE increase (red), and the selected fit width for a single participant

Section surface area and volume were determined by extracting a 75mm (3") section from the point cloud which was then bound with a triangulated shape object in MATLAB, which returned volume and surface area. The section width of 3" was selected because it was the maximum length available for all participants and corresponded closely to the length of the short brace.

Four geometric parameters – radius of curvature, surface area, section volume, and maximum cross-sectional area – were calculated from the 3" section. These parameters were correlated to the maximum force sustained in each test with Pearson correlation coefficients. Pain scores and maximum interface forces were subdivided by brace for correlation to these geometric parameters (also using Pearson coefficients). Although participants reported pain scores on half-points on the NRS, pain data was still technically ordinal (requiring Spearman's Rho to find relationships with geometry). However, treating pain scores as continuous data allowed for Pearson's correlations with geometric parameters to be determined using the same assumptions

of linearity and distribution as interface force data. This approach was selected in the interest of consistency across results.

6.3 Results

Correlation coefficients were determined relating maximum interface force to geometric parameters. Interface force was subdivided by brace for this analysis. Radius of curvature had strongest correlations with maximum interface force (ranging from 0.538 to 0.770), whereas all other geometric parameters had medium to strong negative correlations with maximum interface force across brace types (coefficients ranging from -0.336 to -0.683). These correlations are summarized in Table 5.1

Table 5.1: Pearson coefficients correlating geometric parameters and brace performance

	Maximum Applied Load			Maximum Interface Force		
	3" Brace	7" Brace	Mixed Brace	3" Brace	7" Brace	Mixed Brace
Radius of Curvature	0.466	0.376	0.389	0.77**	0.718**	0.538**
Maximum Cross-Sectional Area	-0.032	0.372	0.091	-0.547**	-0.336*	-0.503*
Section Volume	-0.166	0.273	-0.054	-0.628**	-0.434*	-0.588**
Section Surface Area	-0.222	0.215	-0.092	-0.683**	-0.489*	-0.61**

*p<0.05 **p<0.001

6.4 Discussion

Brace failure for one participant raised interest in the interplay of leg geometry and interface force. Geometric analysis of the shapes of the participants' lower legs provided some insight as to why the 7" and mixed designs were not effective for this participant. It was observed during testing that this participant had a nearly cylindrical lower leg with little to no curvature (corresponding to a high radius of curvature across the surface of the leg). Pearson's correlation coefficients were determined relating the leg's radius of curvature and other geometric parameters to the load bearing and interface forces of the different braces. While these parameters did not significantly correlate with the maximum effective load, there were consistent

relationships to the maximum interface force for all braces. Radius of curvature had a positive relationship with maximum interface force where the other parameters all had negative correlation coefficients.

We believe the orientation of the leg surface with respect to the applied load was the root of this relationship – the more aligned the leg surface was to the direction of loading, the less the proportion of applied load that is normal to the leg surface. The normal force component is directly related to the maximum friction force that will adheres the knee brace to the leg. Although all knee braces had similar preload to adhere the brace, the shape of the leg will ultimately determine the traction load at which friction is overcome and whether the brace slips.

7 Discussion

7.1 Overview of Findings

The objectives of this research were to: 1) design lower-leg knee braces that can apply traction load to the knee; and 2) test these prototype knee brace components and relate traction load to wearer discomfort and interface force. These objectives were met in this research through the development of a hypothesis using a simple FE model, the iterative design of a lower leg knee brace, and a pilot study using a mechanical apparatus to test prototypes of the lower leg knee brace.

Testing of the prototype knee braces demonstrated their capability to deliver traction load into the body, thus satisfying Objective 1. The traction forces applied to the braces over the course of our testing well exceeded 10kg of equivalent weight across all participants and brace designs. Most participants saw forces up to 225N, often approaching ½ their bodyweight.

Self-reported pain demonstrated a statistically significant difference among the brace designs. Applied force was demonstrated to significantly increase self-reported pain. This finding is intuitive – any significant increase in force passing through the body will cause some level of discomfort. Among the designs, the mixed and 7” designs were the most comfortable. That both longer models were equally comfortable was a surprise. These results indicate that increasing covered area is important for distributing load and improving comfort where the posterior side is less so. Of note, there was a small, non-significant difference between the 7” and mixed brace designs. It may be that the distal side of the calf muscle body carries more load than the anterior surface of the leg, thereby explaining this small difference.

In support of this premise, the interface measures indicated that the distal-anterior sectors of the 7” knee began to carry more load than in the mixed design, in addition to the load carried from preload in the distal-posterior sectors. It appears from these profiles that the distal-posterior sectors will support large load when present.

Surprisingly, this study did not observe a relationship between maximum interface force and self-reported pain. Qualitative feedback from participants suggests that this may be due to pain concentration at the edges of the brace components rather than a cumulative effect from force

distributed across the body of the brace. Both pain and interface force in the sensor areas were observed to increase overall as the applied traction load increased, but the relationship between these responding variables is unclear. We believe that higher forces must be occurring at the locations indicated verbally by participants – measurements of interface force at these locations may provide a more representative correlation with pain.

Our experimental results support the hypothesis developed in Chapter 4 with the FE model, in that the shorter knee brace performs poorly compared to the longer designs. However, the comparison of the 7" brace to the mixed design contradicts the hypothesis. The mixed design offered similar interface forces and pain levels, and was also lighter and less bulky.

7.2 Comparison to Existing Findings

To the best of our knowledge, no other study has examined OA knee braces using an external testing apparatus to measure traction force. Comparisons of this study to other findings and standards are then limited to analogy rather than direct comparison.

Other lower leg knee braces are abundant and are often formed using casting methods similar to that employed in our design[52]. These knee braces have an abundance of applications that usually focus on providing support, assisting gait, or correcting alignment. OA knee braces typically do not apply force over large areas of the knee, instead applying opposing loads over smaller regions through stiff, light frames. The designs proposed through this research are an amalgam of what has been learned through different areas of orthotics design, directed specifically at solving the problem of applying large traction loads. The distraction/traction knee brace proposed employs casting materials similar to polymer interfaces but is divided into stiff anterior and posterior sections similar to an OA unloader knee brace.

Previous studies have investigated interface mechanics and pain responses using predictive models[39,40]. These models took pressure pain threshold (PPT) measurements of individuals before determining interface stresses using a subject-specific FE model. Our study attempted to employ direct measurement of interface pressures in comparison to an overall pain rating (rather than a series of site-specific PPTs). Our study did not take site-specific PPT values for comparison, choosing instead to examine of load distribution across the surface. A direct connection between site-specific PPT values and the self-reported discomfort or interface forces

of this study is not clear. The next step in connecting our work to these studies would be to relate all three of interface force measures, PPT, and the overall comfort rating. However, this level of detail is outside the scope of our pilot study.

7.3 Strengths and Limitations

The main strength of this research is its novelty. Here, current design ideas from the orthotics industry were adapted to design a lower leg knee brace component that can apply a new kind of load to the body. A testing procedure was then developed that could apply this load to new prototypes. This test method can detect differences in comfort and interface forces among brace designs and can directly contribute to the validation of future design models and investigation of biomechanical interfaces.

The primary limitation of this research is the small sample size of the pilot study. As previously discussed, this small sample size limited the statistical significance of the study results. Further, brace order was not controlled for or randomized between trials within a single participant (thereby limiting the statistical power of the results). Despite these limitations, our research was able to show high-level differences between the braces. At this early stage in design development, trends in this data are sufficient to prompt further investigation using more refined designs and higher-resolution measures.

Modifications to the experimental design will improve the ability of the test method to detect differences among braces. In comparing knee braces, a randomized cross-over design should be used to randomize the order in which participants wear braces to reduce the potential for intra-participant effects (such as building of pain tolerance or shifting in position to increase comfort). Standardization of preload using interface force measures (rather than relative position between brace pieces) may reduce variance in interface force among participants but such a standard is not immediately apparent, as interface forces were shown to correlate strongly with individual leg shape and their relationships with participant pain are not yet clear.

The goal of the designed knee brace is to provide distraction to the knee joint but no measures of distraction were taken in this research. This study is, to the best of our knowledge, the first to assess the load-bearing capability of a rigid knee brace. While previous studies have used short-term loading to unload knees, this study applied increasing traction loads to observe an effect

(pain and interface force). Surface palpitations or radiographs may have been used to observe increases in JSW but these changes would be small – attempting distraction on the scale of millimeters in a short period drastically increases the risk of rupturing ligaments and tendons. This pilot study was needed to assess the feasibility and safety of applying traction load through the rigid lower-leg knee brace in low-level increments of load. To measure distraction, a longer-term test is required which, in turn, necessitates the completed knee brace design.

8 Conclusions and Future Directions

8.1 Conclusions

First, this research provides a viable design for a lower-leg traction knee brace and demonstrates the brace's capability to provide traction loading in excess of 1/3rd of the wearer's bodyweight, thus fulfilling Objective 1. Objective 2 has also been fulfilled through the pilot testing described in this thesis. Relationships between load and wearer discomfort were found through this test and were found to be dependent on brace design. Relationships fulfilling Objective 2 distinguished between a 3" design, a 7" design, and a mixed design. This test demonstrated a difference in performance, with the 3" design being the least effective and the 7" and mixed designs the most effective.

8.2 Contributions

The contributions of this work begin with a proven design concept and prototypes for a lower-leg traction knee brace and providing evidence of their capability to distribute load into the leg. This design provides a foundation for future designs that may succeed in providing non-surgical distraction of the knee joint.

This work also provides a methodology for testing the lower-leg components of new knee brace designs. Differences in brace comfort and interface behavior can be detected with this method, providing a useful tool for validating and further optimizing brace designs. Superior brace designs (the mixed and 7" designs) have already been selected using this method.

Finally, this work provides a comparison of three simple designs that highlights the importance of surface area coverage, traction, and mechanical compliance, thereby providing grounds for the immediate refinement of the design.

8.3 Clinical Significance

This research will contribute to clinical practice by guiding the design of highly-effective devices for the treatment of OA. Using this research as a foundation, knee braces can be designed that will be able to load the knee in traction without the need for surgical devices. At sufficiently high magnitudes, this traction load will provide non-invasive distraction of the knee. This research

then provides an important utility in expanding research into the effects of knee joint distraction in reversing the effects of OA.

8.4 Recommendations for Future Research

This research was aimed at piloting investigation into high-load traction knee braces. Next steps for investigation in this area should be focused on the continued optimization and completing the design. The results from this study suggest that one improvement could be to improve fit and comfort near the edges of the brace. Reducing the stiffness of the brace near the edges would reduce the painful pinching sensation reported by participants in this study.

Improvements on the current design will also need to be studied and validated, using similar methods to those employed in this study. A high-resolution sensor could provide sufficient resolution to more closely observe shifts in load distribution across brace interfaces. This higher resolution would also provide basis for comparison between PPT values and the overall score given in this study. Data from this study, specifically variances and means of self-reported pain and interface forces, can be used to estimate effect sizes and determine statistical power for future studies.

Finally, this research should be expanded to include an upper-leg interface and loading mechanism. The rigid fiberglass design presented here can be adapted to the upper leg, provided that attention is given to the greater presence of soft tissue in the upper leg. An even greater surface of the upper leg may need to be covered to comfortably transfer load. Increasing this area may also require the point of force application to be moved away from the knee joint (reducing the effect of moments on shifting load away from the knee).

8.5 Closing Remarks

This research seeks to establish a foundation for the future development of traction-distraction knee braces to treat osteoarthritis. The lower-leg component of such a knee brace has been designed and tested on a small population of healthy participants. It has been shown that the mechanical testing method presented in this study identified relationships among traction load, interface force, and wearer comfort. Presently these relationships are general in nature but a method has been established that can be used to delve more deeply into interface biomechanics.

This study has shown the importance of moving towards the customizable, quantitative, and mindfully-optimized design of high-performance orthotics.

References

1. Measure Description – Percentage of population with diagnosed osteoarthritis [web document]. Government of Canada – Canadian Chronic Disease Indicators. Published September 19th, 2016.
2. McAlindon TE, Bannuru RR, Sullivan MC, Arden NK, Berenbaum F, Bierma-Zeinstra SM, et al. OARSI guidelines for the non-surgical management of knee osteoarthritis. Osteoarthr Cartil. 2014; 22(3):363–88.
3. Intema F, Van Roermund M. P, Marijnissen ACA, Cotofana S, Eckstein F, Castelein RM, et al. Tissue structure modification in knee osteoarthritis by use of joint distraction: an open 1-year pilot study. Ann Rheum Dis. 2011; 70(8):1441.
4. Wiegant K, van Roermund PM, Intema F, Cotofana S, Eckstein F, Mastbergen SC, et al. Sustained clinical and structural benefit after joint distraction in the treatment of severe knee osteoarthritis. Osteoarthr Cartil. 2013; 21(11):1660–7.
5. van der Woude J, Wiegant K, van Roermund PM, Intema F, Custers RJH, Eckstein F, et al. Five-Year Follow-up of Knee Joint Distraction. Cartilage. 2016; 8(3): 263-71.
6. Squyer E, Stamper DL, Hamilton DT, Sabin JA, Leopold SS. Unloader knee braces for osteoarthritis: Do patients actually wear them? Clin Orthop Relat Res. 2013.
7. Stammen K. Human Knee Anatomy.jpg. Wikimedia Commons (free image repository) [Internet]. 2012. Accessed March 13th, 2018.
8. Bijlsma JWJ, Berenbaum F, Lafeber FPJG. Osteoarthritis: an update with relevance for clinical practice. Lancet. 2016 Nov; 377(9783):2115–26.
9. Kellgren JH, Lawrence JS. Radiological Assessment of Osteo-Arthrosis. Ann Rheum Dis. 1957; 16(4):494 LP-502.
10. Sato T, Sato N, Masui K, Hirano Y. Immediate Effects of Manual Traction on Radiographically Determined Joint Space Width in the Hip Joint. J Manipulative Physiol Ther. 2014; 37(8):580–5.
11. Ogawa D, Usa H, Abiko T, Matsumura M, Ichikawa K, Hata M, et al. Analysis of separation distance that accompanies the continuous traction of normal knee joints using ultrasound imaging. Physiotherapy. 2015; 101:e1120.

12. Khademi-Kalantari K, Mahmoodi Aghdam S, Akbarzadeh Baghban A, Rezayi M, Rahimi A, Naimee S. Effects of non-surgical joint distraction in the treatment of severe knee osteoarthritis. J Bodyw Mov Ther. 2014; 18(4):533–9.
13. van Valburg AA, van Roermund PM, Marijnissen ACA, van Melkebeek J, Lammens J, Verbout AJ, et al. Joint distraction in treatment of osteoarthritis: a two-year follow-up of the ankle. Osteoarthr Cartil. 1999; 7(5):474–9.
14. Van Valburg AA, Van Roermund PM, Marijnissen ACA, Wenting MJG, Verbout AJ, Lafeber FPJG, et al. Joint distraction in treatment of osteoarthritis (II): effects on cartilage in a canine model. Osteoarthr Cartil. 2000; 8(1):1–8.
15. Brooks KS. Osteoarthritis Knee Braces on the Market: A Literature Review. JPO J Prosthetics Orthot. 2014; 26(1): 2-30.
16. Brouwer RW, van Raaij TM, Verhaar JAN, Coene LNJEM, Bierma-Zeinstra SMA. Brace treatment for osteoarthritis of the knee: a prospective randomized multi-centre trial. Osteoarthr Cartil. 2006; 14(8):777–83.
17. Duivenvoorden T, Brouwer RW, van Raaij TM, Verhagen AP, Verhaar JAN, Bierma-Zeinstra SMA. Braces and orthoses for treating osteoarthritis of the knee. Cochrane Database Syst Rev. 2015.
18. Steadman R, Briggs K, Pomeroy S, Wijdicks C, Briggs KK, Pomeroy SM, et al. Current state of unloading braces for knee osteoarthritis. Knee Surgery, Sport Traumatol Arthrosc. 2016; 24(1):42–50.
19. Petersen W, Ellermann A, Zantop T, Rembitzki I, Semsch H, Liebau C, et al. Biomechanical effect of unloader braces for medial osteoarthritis of the knee: a systematic review. Arch Orthop Trauma Surg. 2016; 136(5):649–56.
20. Maleki M, Arazpour M, Joghtaei M, Hutchins SW, Aboutorabi A, Pouyan A. The effect of knee orthoses on gait parameters in medial knee compartment osteoarthritis A literature review. Prosthet Orthot Int. 2016; 40(2):193–201.
21. Moyer R., Birmingham TB, Bryant DM, Giffin JR, Marriott K., Leitch KM. Biomechanical effects of valgus knee bracing: a systematic review and meta-analysis - ScienceDirect. Osteoarthr Cartil. 2015; 23(2):178–88.
22. Horlick SG, Loomer RL. Valgus Knee Bracing for Medical Gonarthrosis. Clin J Sport Med. 1993; 3(4):251–5.

23. Richards JD, Sanchez-Ballester J, Jones RK, Darke N, Livingstone BN. A comparison of knee braces during walking for the treatment of osteoarthritis of the medial compartment of the knee. J Bone Joint Surg Br. 2005; 87(7):937–39.
24. Jones RK, Nester CJ, Richards JD, Kim WY, Johnson DS, Jari S, et al. A comparison of the biomechanical effects of valgus knee braces and lateral wedged insoles in patients with knee osteoarthritis. Gait Posture. 2013; 7(3):368–72.
25. Haladik J, Vasileff W, Peltz C, Lock T, Bey M. Bracing improves clinical outcomes but does not affect the medial knee joint space in osteoarthritic patients during gait. Knee Surgery, Sport Traumatol Arthrosc. 2014; 22(11):2715–20.
26. Gaasbeek RDA, Groen BE, Hampsink B, van Heerwaarden RJ, Duysens J. Valgus bracing in patients with medial compartment osteoarthritis of the knee: A gait analysis study of a new brace. Gait Posture. 2007; 26(1):3–10.
27. Laroche D, Morisset C, Fortunet C, Gremeaux V, Maillefert J-F, Ornetti P. Biomechanical effectiveness of a distraction–rotation knee brace in medial knee osteoarthritis: Preliminary results. Knee. 2014; 21(3):710–6.
28. Draganich L, Reider B, Rimington T, Piotrowski G, Mallik K, Nasson S. The effectiveness of self- adjustable custom and off-the- shelf bracing in the treatment of varus gonarthrosis. J bone Joint surgery American 2006; 88(12):2645.
29. Della Croce U, Crapanzano F, Li L, Kasi PK, Patritti BL, Mancinelli C, et al. A Preliminary Assessment of a Novel Pneumatic Unloading Knee Brace on the Gait Mechanics of Patients With Knee Osteoarthritis. PM&R. 2013; 5(10):816–24.
30. Pollo FE, Otis JC, Backus SI, Warren RF, Wickiewicz TL. Reduction of medial compartment loads with valgus bracing of the osteoarthritic knee. Am J Sports Med. 2002; 30(3):414–21.
31. Johnson AJ, Starr R, Kapadia BH, Bhave A, Mont MA. Gait and clinical improvements with a novel knee brace for knee OA. J Knee Surg. 2013; 26(03):173–8.
32. Hart H, Collins N, Ackland D, Cowan S, Crossley K. The effects of varus bracing for predominant lateral knee osteoarthritis and valgus malalignment after ACL reconstruction. J Sci Med Sport. 2014; 18:16–7.

33. Nadaud MC, Komistek RD, Mahfouz MR, Dennis DA, Anderle MR. In vivo three-dimensional determination of the effectiveness of the osteoarthritic knee brace: a multiple brace analysis. J bone Joint surgery American Vol. 2005; 87 Suppl 2:114–9.
34. Pierrat B, Molimard J, Navarro L, Avril S, Calmels P. Evaluation of the mechanical efficiency of knee braces based on computational modeling. Comput Methods Biomech Biomed Engin. 2015; 18(6):646–61.
35. Dickinson AS, Steer JW, Worsley PR. Finite element analysis of the amputated lower limb: A systematic review and recommendations. Med Eng Phys. 2017; 43:1–18.
36. Buis AW, Convery P. Calibration problems encountered while monitoring stump/socket interface pressures with force sensing resistors: techniques adopted to minimize inaccuracies. Prosthet Orthot Int. 1997; 21(3):179.
37. Convery P, Buis AW. Conventional patellar-tendon-bearing (PTB) socket/stump interface dynamic pressure distributions recorded during the prosthetic stance phase of gait of a trans-tibial amputee. Prosthet Orthot Int. 1998; 22(3):193.
38. Al-Fakih EA, Abu Osman NA, Mahamd Adikan FR, Eshraghi A, Jahanshahi P. Development and Validation of Fiber Bragg Grating Sensing Pad for Interface Pressure Measurements Within Prosthetic Sockets. IEEE Sens J. 2016; 16(4):965–74.
39. Wu C, Chang C, Hsu A, Lin C, Chen S, Chang G. A proposal for the pre-evaluation protocol of below-knee socket design - integration pain tolerance with finite element analysis. J Chinese Inst Eng. 2003; 26(6):853–60.
40. Lee WCC, Zhang M. Using computational simulation to aid in the prediction of socket fit: A preliminary study. Med Eng Phys. 2007; 29(8):923–9.
41. Lacroix D, Ramírez Patiño JF. Finite element analysis of donning procedure of a prosthetic transfemoral socket. Ann Biomed Eng. 2011; 39(12):2972–83.
42. Polyethylene (PE). CES Edupack 2017. Produced by Granata Design.
43. Kosek E, Ekholm J, Nordemar R. A comparison of pressure pain thresholds in different tissues and body regions. Long-term reliability of pressure algometry in healthy volunteers. Scandinavian journal of rehabilitation medicine. 1993; 25:117-124.
44. Zhang WJ, Lin Y, Sinha N. On the function-behaviour-structure model for design. Proceedings of the Canadian Engineering Educators Assoc. 2011.

45. BSN Medical. Delta-Lite Plus [webpage]. 2018. Accessed May 29, 2018. Available from: http://www.bsnmedical.com/products/orthopaedics/category-product-search-o/fracture-management/synthetic-casting/delta-liter-plus.html
46. Hall RS, Desmoulin GT, Milner TE. A technique for conditioning and calibrating force-sensing resistors for repeatable and reliable measurement of compressive force. J Biomech. 2008; 41(16):3492–5.
47. Williamson A, Hoggart B. Pain: a review of three commonly used pain rating scales. J Clinical Nursing. 2005: 14(7):798-804
48. Digilent: a National Instruments company. Waveforms [Software]. 2015. Available from: https://store.digilentinc.com/waveforms-previously-waveforms-2015/
49. NextEngine. ScanStudio Proscan [Software]. 2018. Available from: https://www.nextengine.com/products/scanstudio-hd/specs/overview
50. 3D Systems. Geomagic Studio 14 [Software]. 2014. No longer available. Product updates available from: https://www.3dsystems.com/software
51. Tuszynski J. Surface Intersection, version 1.0 [Software]. 2014. Accessed March 14, 2018. Available from: https://www.mathworks.com/matlabcentral/fileexchange/48613-surface-intersection
52. Chernov N. Circle Fit (Pratt method) [Software]. 2009. Accessed March 14, 2018. Available from: https://www.mathworks.com/matlabcentral/fileexchange/22643-circle-fit--pratt-method-
53. Hsu JD, Michael JW, Fisk 1943- JR, Surgeons AA of O. AAOS atlas of orthoses and assistive devices. 4th ed.. Philadelphia: Philadelphia : Mosby/Elsevier; 2008.

Appendix A. Von Mises Stress Contours from Planar FE Simulation

Default settings for this finite element (FE) simulation were in Imperial units. Results from this simulation are shown in thousands of pounds per inch (ksi). The von Mises stresses are contoured through all three bodies for brace coverage in length ratios (LR) from 0.05 to 0.99 of the line defining the lower calf.

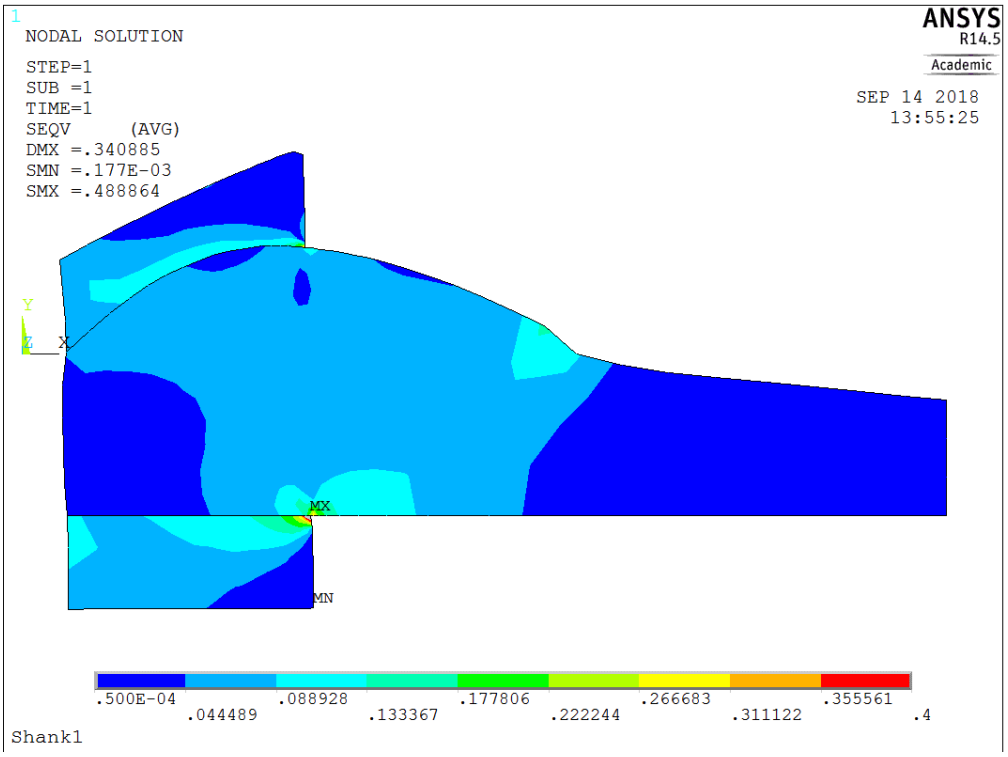

Figure A.1: Von Mises stress contour plot for LR 0.05

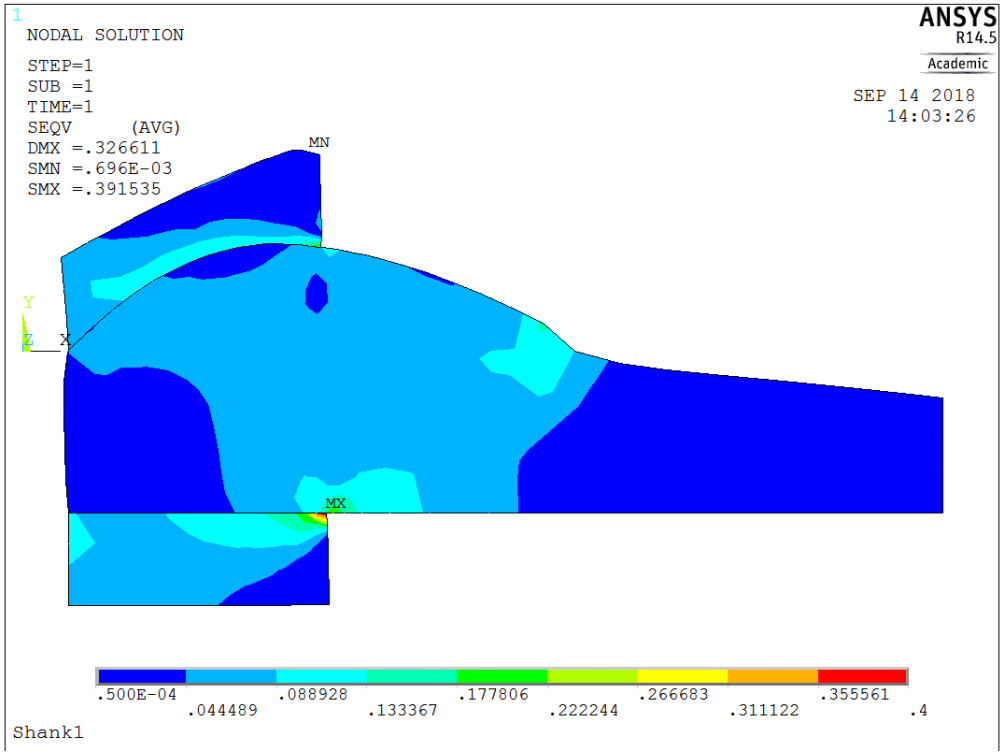

Figure A.2: Von Mises stress contour plot for LR 0.10

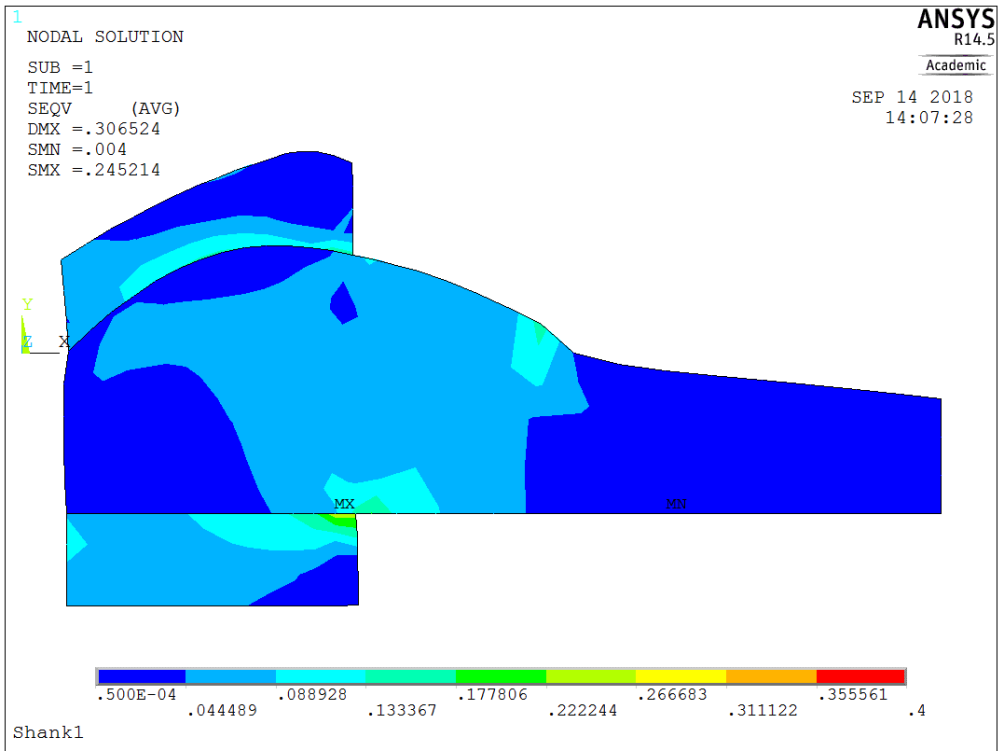

Figure A.3: Von Mises stress contour plot for LR 0.20

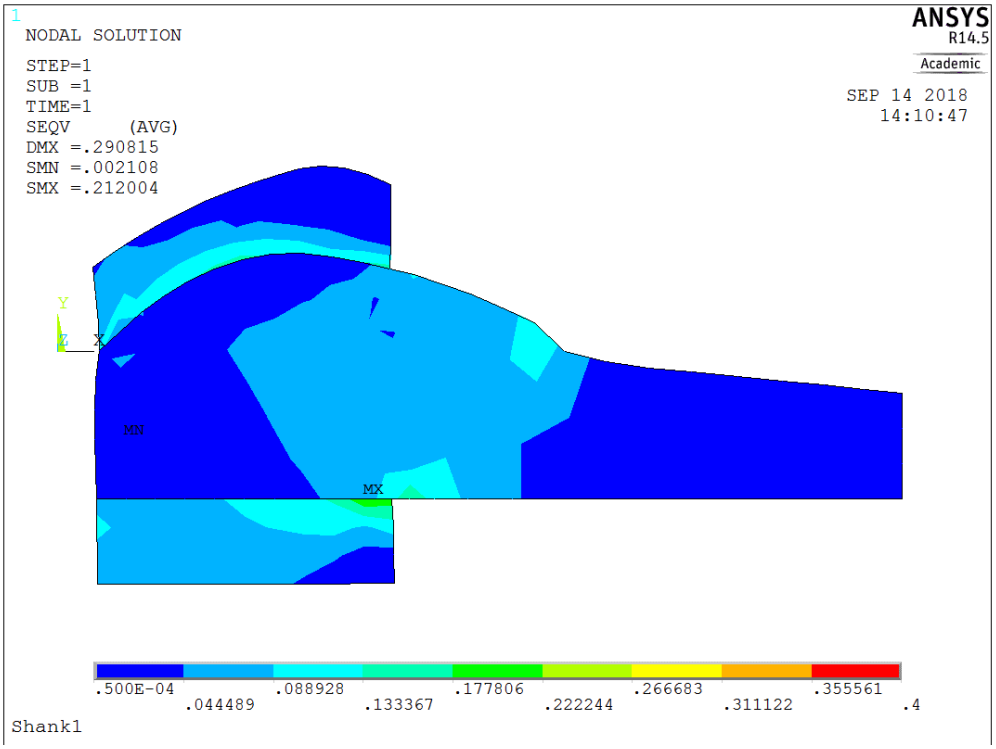

Figure A.4: Von Mises stress contour plot for LR 0.30

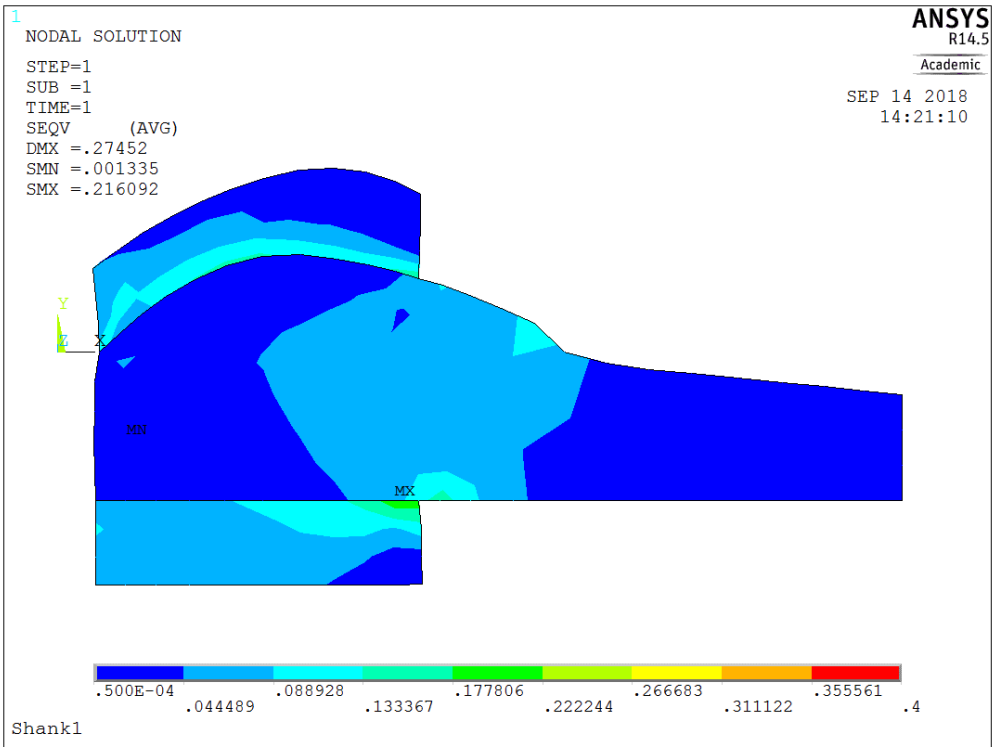

Figure A.5: Von Mises stress contour plot for LR 0.40

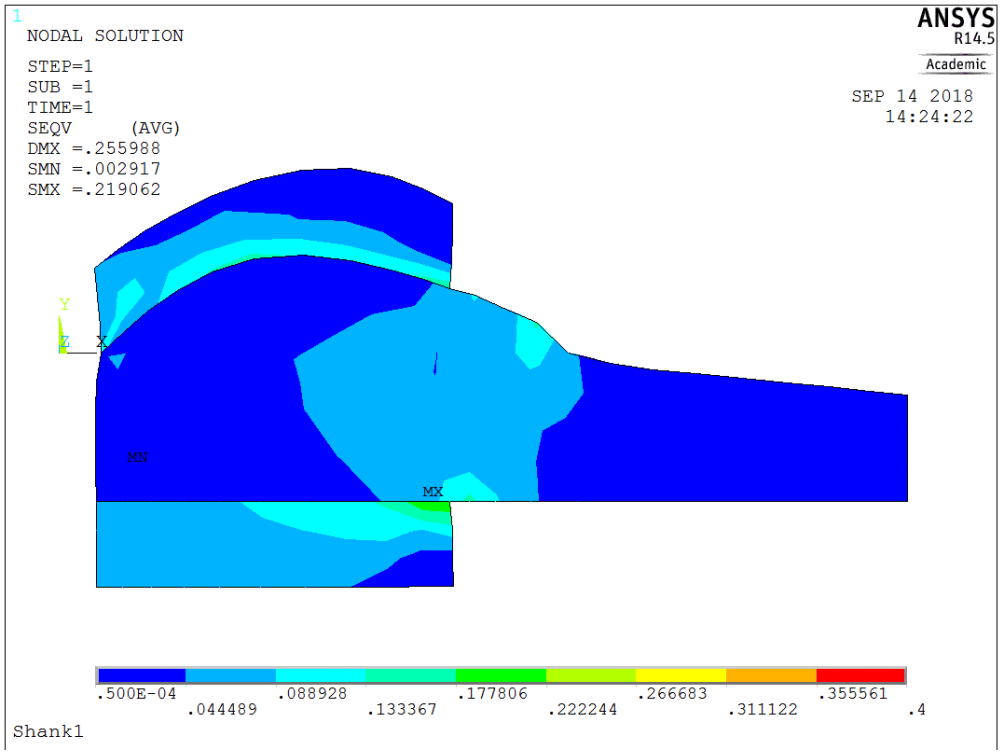

Figure A.6: Von Mises stress contour plot for LR 0.50

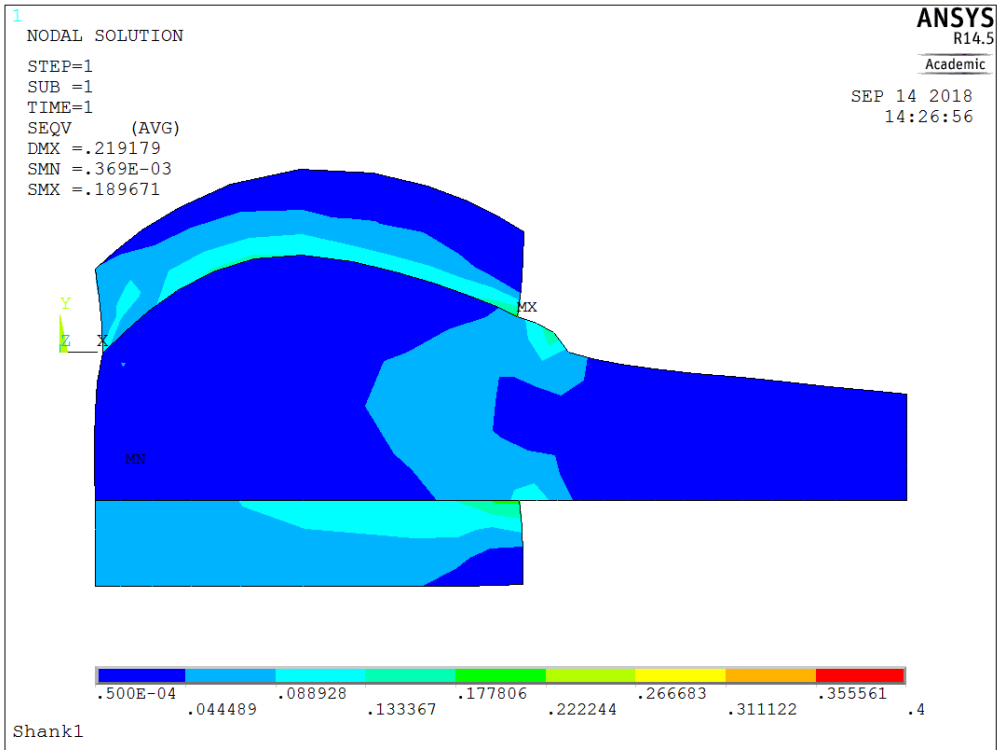

Figure A.7: Von Mises stress contour plot for LR 0.75

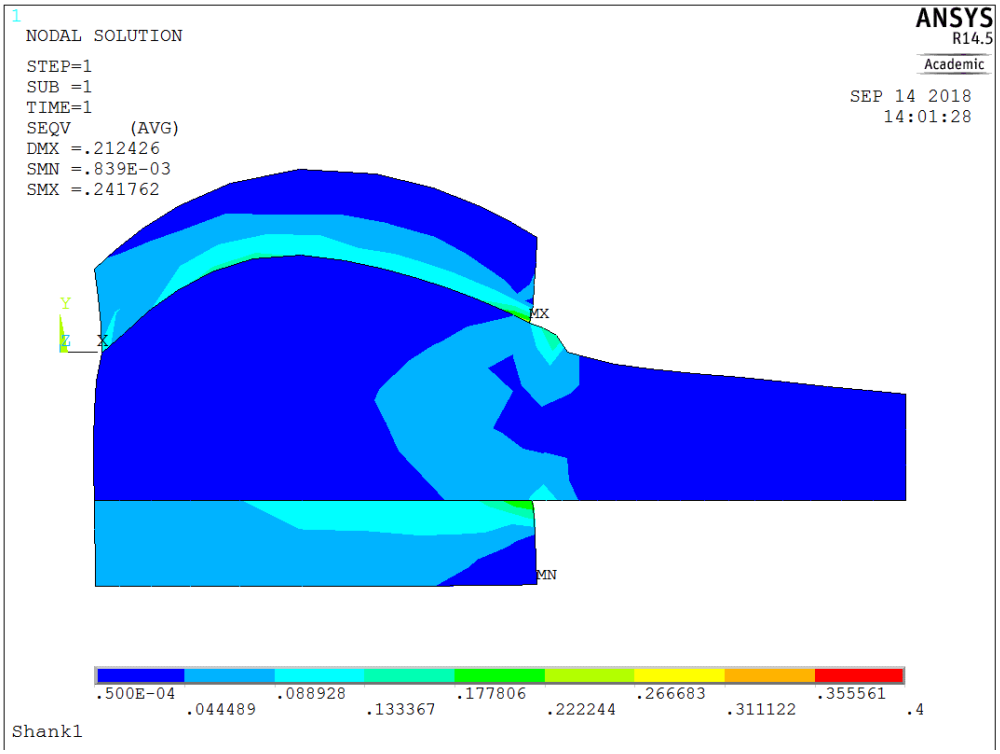

Figure A.8: Von Mises stress contour plot for LR 0.80

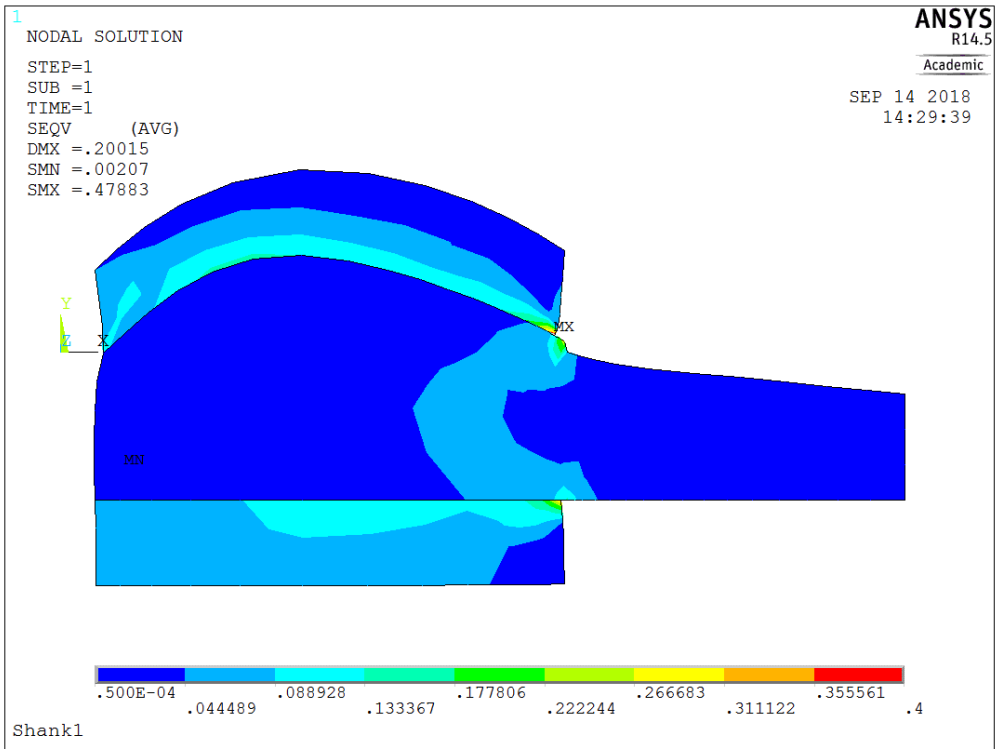

Figure A.9: Von Mises stress contour plot for LR 0.99

Appendix B. Participant Information and Subject-Specific Test Data

This document contains participant-specific data obtained during testing and post-hoc geometric analysis of participants' leg geometry. Characteristic information (bodyweight, leg geometry) for all participants is reported in Table B.1. The remaining tables summarize test data by participant for all three knee braces.

Table B.1: Summary of Participant Charateristics

Participant	Sex	Bodyweight [lb]	Radius of Curvature [mm]	Maximum Cross-Sectional Area [mm^2]	3" Section Volume [mm^3]	3" Section Surface Area [mm^2]
246145	F	139	281.3	1.0651	838300	27650
345024	F	181	171.4	1.4638	1053000	30680
631450	M	152	244	1.06282	757900	26760
694828	M	263	590.3	1.8053	1309000	34760
814723	F	127	511.1	1.0041	709800	25080
867530	M	214	340.8	1.3796	973500	29560
520016	M	231	278.3	1.625	1173000	32220

Table B.2: Test Data for Participant 246145

3" Brace	Load	Interface Forces [N]								Pain
	[N]	Q1	Q2	Q3	Q4	Q5	Q6	Q7	Q8	Rating
	0.0	64.2	47.8	18.2	4.1					1
	58.7	60.5	35.3	18.6	4.2					3
	88.1	57.9	22.5	18.1	4.1					5
	117.4	64.2	8.6	18.1	4.1					6
	146.8	58.7		18.1	4.1					6.5
7" Brace	**Load**	**Interface Forces [N]**								**Pain**
	[N]	**Q1**	**Q2**	**Q3**	**Q4**	**Q5**	**Q6**	**Q7**	**Q8**	**Rating**
	0.0	33.1	19.7	28.8	18.0	16.8	9.8	21.6	37.6	0.5
	58.7	31.5	24.5	27.9	18.0	28.0	28.8	24.5	54.3	1
	88.1	37.9	33.3	32.4	18.0	35.4	28.8	28.9	59.1	2
	117.4	84.5	33.7	19.7	18.0	19.6	28.5	32.5	89.7	3
	146.8	23.0	15.2	16.7	18.0	16.8	11.5	24.8	40.2	4.5
	176.1	63.2	14.8	18.2	18.0	18.2	8.7	21.4	71.2	5.5
Mixed	**Load**	**Interface Forces [N]**								**Pain**
Brace	**[N]**	**Q1**	**Q2**	**Q3**	**Q4**	**Q5**	**Q6**	**Q7**	**Q8**	**Rating**
	0.0	37.3	22.7	43.2	18.0	16.5	7.2			0.5
	58.7	13.3	17.7	25.8	18.0	16.6	20.3			3
	88.1	28.5	32.9	4.4	18.0	16.5	25.2			5.5
	117.4	23.0	40.5	3.4	18.0	17.1	33.2			6.5
	146.8	22.9	42.7		18.0	20.3	44.4			6.5

Table B.3: Test data for Participant 345024

	Load	Interface Forces [N]								Pain
3" Brace	**[N]**	**Q1**	**Q2**	**Q3**	**Q4**	**Q5**	**Q6**	**Q7**	**Q8**	**Rating**
	0.0	0.0	11.0	20.3	4.6					0.0
	58.7	2.4	25.8	13.4	4.3					1.0
	88.1	3.4	25.8	16.8	5.8					3.0
	117.4	3.1	23.9	15.6	5.2					3.0
	146.8	6.0	23.4	10.6	5.5					4.0
	176.1	52.0	30.0	6.5	5.3					5.0
	205.5	10.5	34.4	3.7	4.5					6.0
	Load	**Interface Forces [N]**								**Pain**
7" Brace	**[N]**	**Q1**	**Q2**	**Q3**	**Q4**	**Q5**	**Q6**	**Q7**	**Q8**	**Rating**
	0.0	0.4	7.5	4.1	4.0	3.7	1.6	8.6	3.6	1.0
	58.7	2.9	12.3	7.3	4.0	3.7	1.6	15.5	12.4	2.0
	88.1	0.3	14.9	12.6	4.1	3.7	1.6	26.3	9.2	3.0
	117.4	0.4	62.4	26.4	4.1	3.7	1.6	31.7	22.5	4.0
	146.8	1.2	21.8	9.2	4.1	3.8	1.6	37.0	26.5	5.5
	176.1	1.9	31.3	11.2	4.1	3.8	2.5	36.2	30.8	6.0
	205.5	8.8	25.3	12.2	4.1	3.8	2.7	24.3	20.4	6.5
	Load	**Interface Forces [N]**								**Pain**
Mixed Brace	**[N]**	**Q1**	**Q2**	**Q3**	**Q4**	**Q5**	**Q6**	**Q7**	**Q8**	**Rating**
	0.0	0.1	3.9	2.1	4.0	3.7	1.9			1.0
	58.7	1.7	16.8	6.1	4.8	3.7	2.3			1.0
	88.1	1.6	10.5	5.9	4.3	3.8	1.9			2.0
	117.4	2.1	21.0	2.9	4.8	4.1	2.8			5.0
	146.8	3.5	33.6	4.2	4.4	3.7	1.6			5.0
	176.1	3.1	18.3	0.5	4.3	3.9	2.7			6.0
	205.5	3.8	27.5	0.9	4.0	3.7	1.7			6.5

Table B.4: Test results for Participant 631450

3" Brace	Load	Interface Forces [N]								Pain
	[N]	Q1	Q2	Q3	Q4	Q5	Q6	Q7	Q8	Rating
	0.0	0.0	1.7	8.6	4.1					0.0
	58.7	0.5	4.4	3.7	4.0					0.0
	88.1	2.4	11.6	8.6	4.4					0.0
	117.4	1.2	5.7	4.5	6.0					0.0
	146.8	1.5	5.3	5.8	4.0					0.0
	176.1	2.5	6.5	8.6	4.1					5.0
	205.5	10.3	26.9	16.6	15.7					4.0
	234.9	12.9	27.5	19.5	7.7					4.0
	264.2	19.9	41.2	14.1	7.1					3.0
7" Brace	**Load**	**Interface Forces [N]**								**Pain**
	[N]	**Q1**	**Q2**	**Q3**	**Q4**	**Q5**	**Q6**	**Q7**	**Q8**	**Rating**
	0.0	5.7	14.0	14.8	4.0	3.7	7.5	7.2	2.4	0.0
	58.7	6.4	10.5	8.6	4.3	4.6	5.7	6.6	20.5	0.0
	88.1	5.0	15.6	11.9	4.2	5.4	4.6	8.1	18.4	0.0
	117.4	3.6	19.2	12.8	4.3	6.0	7.1	7.8	17.5	0.5
	146.8	2.3	19.9	14.1	4.4	13.5	8.2	8.2	25.8	1.0
	176.1	18.2	14.0	15.4	4.6	13.3	2.3	6.6	29.1	2.0
	205.5	3.5	25.8	16.6	5.0	41.0	8.2	10.1	37.0	3.0
	234.9	10.3	33.6	22.0	23.1	60.6	41.9	21.9	50.2	4.0
	264.2	6.0	30.0	23.9	18.6	47.5	37.8	21.9	41.8	5.0
Mixed	**Load**	**Interface Forces [N]**								**Pain**
Brace	**[N]**	**Q1**	**Q2**	**Q3**	**Q4**	**Q5**	**Q6**	**Q7**	**Q8**	**Rating**
	0.0	8.4	49.1	23.5	4.4	3.7	1.6			0.0
	58.7	10.5	110.1	37.6	21.2	5.0	1.8			0.0
	88.1	10.7	102.8	27.1	15.1	7.2	1.7			1.0
	117.4	8.7	73.2	19.5	7.3	11.5	1.9			3.0
	146.8	12.7	88.2	20.3	6.2	16.8	1.7			3.5

	176.1	10.0	62.4	19.8	5.9	17.6	1.7	3.0
	205.5	10.2	36.1	14.3	5.0	3.8	1.6	3.0
	234.9	3.0	7.8	8.2	4.1	3.8	1.7	4.0
	264.2	14.8	36.1	15.9	7.3	41.0	2.7	5.0
	293.6	17.8	40.1	20.3	11.5	21.1	5.2	4.0

Table B.5: Test data for Participant 694828

3" Brace	Load	Interface Forces [N]								Pain
	[N]	Q1	Q2	Q3	Q4	Q5	Q6	Q7	Q8	Rating
	0.0	5.2	8.7	5.2	4.0					0.0
	58.7	8.8	3.5	8.8	4.0					0.0
	88.1	7.3	13.2	7.3	4.0					0.0
	117.4	27.3	17.1	27.3	4.1					0.5
	146.8	25.9	30.6	25.9	4.0					0.5
	176.1	37.6	42.3	37.6	4.7					0.5
7" Brace	**Load**	**Interface Forces [N]**								**Pain**
	[N]	**Q1**	**Q2**	**Q3**	**Q4**	**Q5**	**Q6**	**Q7**	**Q8**	**Rating**
	0.0	6.8	17.1	20.3	4.7	3.7	5.9	4.7	3.2	0.5
	58.7	10.0	13.2	23.9	7.5	3.7	4.2	5.1	1.0	1.0
	88.1	9.0	12.8	25.2	7.9	3.7	5.4	4.9	1.4	2.0
	117.4	7.4	15.3	30.2	5.9	3.7	8.2	4.6	1.2	3.0
Mixed	**Load**	**Interface Forces [N]**								**Pain**
Brace	**[N]**	**Q1**	**Q2**	**Q3**	**Q4**	**Q5**	**Q6**	**Q7**	**Q8**	**Rating**
	0.0	11.5	10.7	9.7	4.1	3.7	8.6			0.0
	58.7	13.9	14.0	18.5	4.2	3.7	11.0			0.0
	88.1	15.4	14.2	18.5	4.3	3.7	7.8			0.0
	117.4	24.0	12.6	20.0	4.3	3.7	4.8			1.0
	146.8	24.0	18.6	23.2	5.7	3.7	1.6			1.0
	176.1	11.5	10.7	9.7	4.1	3.7	8.6			0.0

Table B.6: Test data for Participant 814723

3" Brace	Load	Interface Forces [N]								Pain
	[N]	Q1	Q2	Q3	Q4	Q5	Q6	Q7	Q8	Rating
	0.0	16.4	52.3	26.7	5.9					0.5
	58.7	23.4	67.4	36.9	18.6					2.5
	88.1	24.6	70.2	39.7	15.7					3.0
	117.4	25.2	68.7	39.0	17.9					3.5
	146.8	23.4	70.2	42.1	17.8					3.5
	176.1	23.4	70.2	42.9	18.6					3.5
	205.5	25.2	73.2	42.9	21.2					4.0
	234.9	28.0	73.2	42.1	21.2					4.5
	264.2	26.6	73.2	41.3	22.1					4.5
	283.3	25.2	70.2	40.5	22.1					4.5
7" Brace	**Load**	**Interface Forces [N]**								**Pain**
	[N]	**Q1**	**Q2**	**Q3**	**Q4**	**Q5**	**Q6**	**Q7**	**Q8**	**Rating**
	0.0	68.0	25.3	15.9	5.5	6.6	8.2	9.2	37.0	1.0
	58.7	75.5	15.6	19.5	7.9	11.5	10.0	10.5	20.9	1.0
	88.1	71.6	14.9	18.3	6.6	11.0	10.0	11.3	18.1	1.5
	117.4	56.5	12.8	15.0	5.9	8.2	7.8	10.7	18.7	1.5
	146.8	71.6	12.3	14.6	6.3	16.1	11.0	11.1	38.8	2.0
	176.1	79.7	14.2	15.8	5.1	11.5	6.9	12.2	36.2	2.5
	205.5	84.4	11.5	13.3	5.6	13.5	10.0	11.2	20.1	2.5
	234.9	79.7	11.3	15.0	5.5	14.7	7.1	12.4	24.3	3.0
	264.2	75.5	11.4	13.6	5.1	17.6	9.0	12.2	21.3	3.0
	283.3	79.7	11.4	15.6	5.0	16.8	11.0	14.8	23.8	3.0
Mixed	**Load**	**Interface Forces [N]**								**Pain**
Brace	**[N]**	**Q1**	**Q2**	**Q3**	**Q4**	**Q5**	**Q6**	**Q7**	**Q8**	**Rating**
	0.0	13.4	37.1	29.3	7.5	8.0	11.6			0.5
	58.7	16.7	15.6	35.0	10.3	14.1	9.0			1.0
	88.1	17.8	14.9	35.0	9.9	13.5	10.0			1.5

	117.4	16.7	12.8	33.8	8.2	11.9	8.6	1.5
	146.8	16.4	12.3	32.2	8.4	18.4	7.8	2.0
	176.1	15.4	14.2	30.2	8.4	16.1	4.8	2.0
	205.5	15.1	11.5	28.4	43.8	6.3	26.3	2.5
	234.9	16.4	11.3	29.3	9.6	23.1	8.2	2.5
	264.2	16.7	11.4	30.2	11.9	25.4	11.6	3.0
	283.3	18.6	11.4	26.7	12.8	29.1	14.2	3.0

Table B.7: Test data for Participant 867530

	Load	Interface Forces [N]								Pain
3" Brace	**[N]**	**Q1**	**Q2**	**Q3**	**Q4**	**Q5**	**Q6**	**Q7**	**Q8**	**Rating**
	0.0	5.8	7.7	18.1	4.0					1.0
	58.7	5.8	9.5	20.8	4.5					2.0
	88.1	4.5	8.2	19.8	4.0					2.5
	117.4	3.5	4.7	18.8	4.0					3.5
	146.8	4.4	3.6	26.7	4.0					5.0
	176.1	4.3	7.7	19.0	4.0					6.0
	205.5	11.1	13.4	19.8	4.0					6.5
	Load	**Interface Forces [N]**								**Pain**
7" Brace	**[N]**	**Q1**	**Q2**	**Q3**	**Q4**	**Q5**	**Q6**	**Q7**	**Q8**	**Rating**
	0.0	7.1	10.3	18.1	5.4	4.3	9.5	7.5	17.5	0.0
	58.7	6.6	10.0	18.8	4.5	4.0	7.5	6.0	40.7	1.0
	88.1	4.1	9.7	17.2	4.2	5.1	10.5	6.4	15.5	1.5
	117.4	35.3	9.3	17.4	4.3	6.6	10.0	6.4	17.5	2.0
	146.8	75.5	8.6	14.1	4.2	6.6	7.8	9.0	16.0	3.0
	176.1	59.1	9.2	18.1	4.5	8.5	8.2	10.4	15.2	3.5
	205.5	12.0	7.9	17.3	5.6	13.5	15.7	12.0	17.5	4.0
	234.9	3.4	12.6	19.3	7.3	10.2	12.8	11.2	36.2	5.5
	264.2	20.3	14.9	17.6	8.4	21.1	41.9	9.8	16.6	7.0
Mixed	**Load**	**Interface Forces [N]**								**Pain**
Brace	**[N]**	**Q1**	**Q2**	**Q3**	**Q4**	**Q5**	**Q6**	**Q7**	**Q8**	**Rating**
	0.0	2.5	9.1	15.0	4.0	3.7	4.2			0.5
	58.7	33.2	12.3	22.6	4.0	3.8	3.6			1.0
	88.1	79.7	8.4	16.6	5.1	4.4	8.6			1.5
	117.4	24.6	12.1	13.3	4.0	3.8	5.7			2.0

Table B.8: Test data for Participant 520016

3" Brace	Load	Interface Forces [N]								Pain
	[N]	Q1	Q2	Q3	Q4	Q5	Q6	Q7	Q8	Rating
	0.0	6.8	14.0	17.6	4.4					4.0
	58.7	2.9	15.6	23.2	5.2					5.0
	88.1	3.8	14.9	21.4	4.8					4.0
	117.4	2.9	12.8	21.4	4.7					4.0
	146.8	3.6	12.3	26.4	5.2					5.0
	176.1	3.4	14.2	32.7	5.8					6.0
	205.5	3.9	11.5	36.3	6.3					6.0
	234.9	3.2	11.3	38.3	6.9					6.5
	264.2	3.3	11.4	39.0	6.2					7.0
7" Brace	**Load**	**Interface Forces [N]**								**Pain**
	[N]	**Q1**	**Q2**	**Q3**	**Q4**	**Q5**	**Q6**	**Q7**	**Q8**	**Rating**
	0.0	8.7	15.8	18.3	5.5	3.9	21.4	23.1	26.8	3.0
	58.7	7.1	15.6	22.6	7.1	4.1	30.8	9.6	28.5	3.0
	88.1	7.6	14.9	22.6	7.1	4.8	23.8	8.2	24.3	3.0
	117.4	3.9	12.8	22.6	6.4	4.0	20.3	10.2	21.7	4.0
	146.8	4.4	12.3	20.6	5.6	4.0	44.1	9.6	22.9	4.0
	176.1	1.1	14.2	21.1	4.3	5.1	39.8	7.6	26.8	4.5
	205.5	1.2	11.5	22.0	4.7	5.1	41.9	8.0	19.4	5.0
	234.9	2.8	11.3	24.5	4.9	5.7	35.9	9.1	23.4	5.0
	264.2	1.7	11.4	23.5	5.9	5.8	46.5	9.8	23.4	5.0
	293.6	12.9	11.4	48.7	13.4	3.8	12.2		14.0	5.5
	322.9	13.1	11.4	49.8	16.3	3.7	4.8		11.2	6.0
	352.3	22.3	11.4	52.1	16.3	3.7	2.8		3.2	6.5
Mixed	**Load**	**Interface Forces [N]**								**Pain**
Brace	**[N]**	**Q1**	**Q2**	**Q3**	**Q4**	**Q5**	**Q6**	**Q7**	**Q8**	**Rating**
	0.0	1.6	10.7	12.2	4.1	3.7	1.6			0.0
	58.7	1.9	15.6	14.5	4.0	3.7	6.2			1.0

88.1	4.2	14.9	12.3	4.0	3.8	3.5	1.0
117.4	4.4	12.8	12.7	4.0	3.8	3.3	2.5
146.8	8.4	12.3	12.0	9.9	23.1	1.7	3.0
176.1	3.9	14.2	6.7	4.8	3.8	3.2	3.5
205.5	6.0	11.5	6.5	4.0	4.2	4.6	4.5
234.9	10.0	11.3	5.5	4.0	4.5	6.8	5.0
264.2	8.4	11.4	5.3	4.0	4.4	7.1	5.0
293.6	10.2	11.4		4.0	4.8	12.8	5.5